Plant, Cell and Environment (2009) **32**, 380–407 doi: 10.1111/j.1365-3040.2009.01933.x

Physiology and proteomics of the water-deficit stress response in three contrasting peanut genotypes

KAMESWARA RAO KOTTAPALLI[1,2], RANDEEP RAKWAL[3,4], JUNKO SHIBATO[3], GLORIA BUROW[2], DAVID TISSUE[5,6], JOHN BURKE[2], NAVEEN PUPPALA[7], MARK BUROW[1,8] & PAXTON PAYTON[2]

Departments of [1]Plant and Soil Science and [5]Biology, Texas Tech University, Lubbock, TX 79409, USA, [2]United States Department of Agriculture Cropping Systems Research Laboratory, Lubbock, TX 79415, USA, [3]Health Technology Research Center (HTRC), National Institute of Advanced Industrial Science and Technology WEST, Onogawa 16-1, Tsukuba, 305-8569, Japan, [4]Research Laboratory for Biotechnology and Biochemistry (RLABB), Kathmandu, Nepal, [6]University of Western Sydney, Centre for Plant and Food Science, Richmond, NSW 2753, Australia, [7]New Mexico State University Agricultural Science Center, Clovis, NM 88101, USA and [8]Texas Agrilife Research and Extension Center Texas A&M System, Lubbock, TX 79403, USA

ABSTRACT

Peanut genotypes from the US mini-core collection were analysed for changes in leaf proteins during reproductive stage growth under water-deficit stress. One- and two-dimensional gel electrophoresis (1- and 2-DGE) was performed on soluble protein extracts of selected tolerant and susceptible genotypes. A total of 102 protein bands/spots were analysed by matrix-assisted laser desorption/ionization–time-of-flight mass spectrometry (MALDI–TOF MS) and by quadrupole time-of-flight tandem mass spectrometry (Q-TOF MS/MS) analysis. Forty-nine non-redundant proteins were identified, implicating a variety of stress response mechanisms in peanut. Lipoxygenase and 1L-myo-inositol-1-phosphate synthase, which aid in inter- and intracellular stress signalling, were more abundant in tolerant genotypes under water-deficit stress. Acetyl-CoA carboxylase, a key enzyme of lipid biosynthesis, increased in relative abundance along with a corresponding increase in epicuticular wax content in the tolerant genotype, suggesting an additional mechanism for water conservation and stress tolerance. Additionally, there was a marked decrease in the abundance of several photosynthetic proteins in the tolerant genotype, along with a concomitant decrease in net photosynthesis in response to water-deficit stress. Differential regulation of leaf proteins involved in a variety of cellular functions (e.g. cell wall strengthening, signal transduction, energy metabolism, cellular detoxification and gene regulation) indicates that these molecules could affect the molecular mechanism of water-deficit stress tolerance in peanut.

Key-words: 1-DGE; 2-DGE; peanut mini-core; drought.

Correspondence: P. Payton. Fax: +1 806 723 5272; e-mail: paxton.payton@ars.usda.gov

Mention of trademark or proprietary product does not constitute a guarantee or warranty of a product by the United States Department of Agriculture (USDA) and does not imply its approval to the exclusion of other products that may also be suitable.

INTRODUCTION

Legumes are the second most important source of food in the world (FAOSTAT data 2007), and production of peanuts (*Arachis hypogaea* L.) is second only to soybean, with a total global harvests of 34 million tons (FAOSTAT data 2007). The USA produces nearly two million tons of peanuts with an annual worth of $1 billion to farmers and $6 billion to the economy overall (United States Department of Agriculture Data and Statistics 2006). The majority of peanut acreage in the south-western USA is in semi-arid regions with limited potential for irrigation, whereas in the south-eastern USA approximately half of the peanut acreage is grown under rain-fed conditions. While peanuts are moderately adaptive to water-deficit conditions, increased urban water usage, prolonged drought in the southern USA and limited water resources (e.g. rapidly declining water table in Ogallala Aquifer) are threatening sustainable peanut crop production. Reductions in water supply generate water-deficit stress in peanuts and subsequent loss of yield. Annually, US crop losses caused by drought exceed $500 million, and it is estimated that approximately half of that loss could be avoided by genetic improvement for water-deficit stress tolerance (Devaiah *et al.* 2007).

Despite the agronomic and economic impacts of drought, little is known about the molecular mechanisms regulating water stress tolerance in peanuts (Jain, Basha & Holbrook 2001; Luo *et al.* 2005). Our knowledge of the molecular responses to abiotic stress is limited primarily to those associated with changes in transcription (Seki *et al.* 2001; Bray 2002; Drame *et al.* 2007). Candidate genes identified during water stress include transcriptional regulators, signal transduction molecules and genes that protect cells against stress (Seki *et al.* 2001). Two signalling molecules, a serine-rich protein and a leucine-rich protein, were identified in a water stress-tolerant peanut (Devaiah *et al.* 2007). Recently, it was shown that increased accumulation of phospholipase Dα and late embryogenesis abundance (LEA) transcripts may reduce water loss and protect cellular components against

stress damage (Drame *et al.* 2007). These researchers also reported that decreased serine protease expression could delay water stress-induced senescence. However, cellular processes are also regulated by protein–protein interactions, post-translational protein modifications and enzymatic activities that cannot be identified by gene expression studies alone.

Proteomic analyses may, therefore, provide a powerful tool to address biochemical and physiological aspects of plant response to water-deficit conditions. For example, Bhushan *et al.* (2007) identified over 100 proteins implicated in cell wall modification, signal transduction, metabolism and cell defence in the cell wall and extracellular matrix in chickpea exposed to dehydration stress. Evaluation of the mitochondrial proteome in pea indicated the broader induction of defence strategies and less protein damage during exposure to water-deficit stress compared to chilling (Taylor *et al.* 2005). At the whole cell level, Hajheidari *et al.* (2005) identified several key photosynthetic enzymes, including ribulose 1·5-bisphosphate carboxylase/oxygenase (Rubisco), as well as proteins involved in redox regulation, reactive oxygen scavenging, signal transduction and chaperone activity that were responsive to water-deficit stress in sugar beet leaves. In rice leaves, proteomics analysis revealed increased actin depolymerizing factor, an S-like RNase homolog, and Rubisco activase, and down-regulation of isoflavone reductase-like proteins during water stress (Salekdeh *et al.* 2002).

Phenotypic screens of core or mini-core peanut germplasm collections have identified variability in many traits, including resistance to both abiotic and biotic stress factors, and aflatoxin contamination (Isleib *et al.* 1995; Anderson, Holbrook & Culbreath 1996; Holbrook, Wilson & Matheron 1998; Holbrook, Stephenson & Johnson 2000). Variability in plant traits associated with water-deficit stress tolerance has been identified in the ICRISAT mini-core collection (Upadhyaya 2005), but little is known about these traits in the US germplasm. In most cases, physiological traits were not examined, and only a few morphological traits (e.g. root length and final yield) were used to assess stress tolerance (Branch & Kvien 1992; Rucker *et al.* 1995; Holbrook *et al.* 2000). While this approach has occasionally been successful (e.g. C76-16 breeding line; Holbrook *et al.* 2007), initial screens utilizing a primarily yield-based analysis for selection of stress tolerance will reject germplasm that exhibits relatively poor yield under well-watered conditions, but has significant potential for tolerance to water deficit. Therefore, strategies that employ a greater range of factors are more likely to successfully identify tolerant lines.

Bennett *et al.* (2002) demonstrated that an integrated approach to selection for abiotic stress tolerance combining physiological, transcript and protein expression could reveal differences that were not identified using a single method. For example, in sorghum an integrated approach indicated that aluminium tolerance was controlled by a single major gene plus several minor genes (Magalhaes 2006). Although the complex tolerance mechanisms for stresses like heat and water deficit are not likely to be as conclusively resolved, identification of key genes, proteins and physiological responses to these stresses in a large and diverse set of germplasm will substantially improve our ability to select stress-tolerant plants.

In this study, our objectives were to increase our understanding of the molecular mechanisms conferring water-deficit stress tolerance in peanuts and to identify stress-tolerant genotypes. Seventy uniform US mini-core genotypes and seven peanut cultivars were screened for stress tolerance, and 20 genotypes were selected for additional water-deficit stress screening and physiological analyses. We utilized a variety of morphological, physiological and proteomic techniques to examine peanut response to well-watered and water-deficit conditions in an environmentally controlled glasshouse. Key enzymes and structural proteins that may be associated with water-deficit stress tolerance were then identified. These results allow us to associate physiologically significant candidate proteins with water-deficit stress tolerance mechanism in peanuts.

MATERIALS AND METHODS

Seed material and water-deficit stress treatment

We investigated 70 peanut genotypes from a US peanut mini-core collection (Kottapalli *et al.* 2007a) and seven additional cultivars. After initial screening, 20 genotypes, consisting of 17 mini-core genotypes and three check cultivars (Table 1), were selected for further evaluation of water stress tolerance utilizing a chlorophyll fluorescence assay (Burke 2007). Plants were grown from seed in 2 L pots in a glasshouse maintained at an optimal growing temperature (31/27 °C day/night cycle) and natural light conditions;

Table 1. Selected US mini-core genotypes and check cultivars for water-deficit stress screening

Mini-core ID	PI #	Subspecies	Market type
COC038	493581	*fastigiata*	Valenicia
COC041	493631	*fastigiata*	Valenicia
COC050	493717	*fastigiata*	Valenicia
COC068	493880	*fastigiata*	Valenicia
COC149	502040	*fastigiata*	Spanish
COC166	494795	*hypogaea*	Runner
COC208	274193	*hypogaea*	Virginia
COC227	290566	*hypogaea*	Runner
COC249	343384	*fastigiata*	Intermediate
COC277	259851	*hypogaea*	Virginia
COC294	372271	*hypogaea*	Virginia
COC388	162655	*fastigiata*	Spanish
COC408	262038	*fastigiata*	Valenicia
COC477	268806	*fastigiata*	Spanish
COC678	476636	*hypogaea*	Virginia
COC698	372305	*hypogaea*	Virginia
COC703	476432	*fastigiata*	Intermediate
Tamrun OL02	Simpson *et al.* 2006	*hypogaea*	Runner
ICGS-76	Nigam *et al.* 1991	*hypogaea*	Virginia
TMV-2	–	*fastigiata*	Spanish

high-pressure sodium lamps (430 W) were used to maintain a 15/9 h light/dark photoperiod. Plants were watered well and adequately supplied with nutrients. We used a randomized block design with three replicate blocks. During the middle of the reproductive growth stage (67 d after planting), half of the plants were subjected to water-deficit stress by withholding water for 7 d, and half of the plants continued to be well watered. Prior to initiation of the water stress, all plants were watered to saturation and pots were weighed; the pots were covered with a gas-permeable polyethylene sheet (ULINE, Chicago, IL, USA) to prevent evaporative water loss from the soil. After 7 d, stressed plants were rewatered to saturation; on average, stressed plants used 62% of the available soil moisture. Leaves were harvested and immediately frozen in liquid nitrogen and stored at –80 °C until further analysis.

Chlorophyll fluorescence screen for stress tolerance

A novel stress bioassay was conducted using a modified chlorophyll fluorescence technique described by Burke (2007). Briefly, leaf samples were collected in the glasshouse before dawn at the end of the water stress treatment (i.e. 7 d after water was withheld), and initial chlorophyll fluorescence yield (F_v/F_m) measurements were conducted using an Opti-Science OS1-FL Modulated Fluorometer (Opti-Sciences, Inc., Hudson, NH, USA). Subsequently, samples were maintained in a growth cabinet (40 °C) in the dark, and F_v/F_m was measured at 8, 24, 32, 48 and 72 h after incubation. The decline in F_v/F_m over time was used as an indicator of the level of stress experienced by the plants prior to incubation. In theory, leaves respire until they exhaust stored carbon reserves present at the time of leaf sampling. Hence, a slow decline in F_v/F_m reflected greater carbon reserves at initial sampling, which was indicative of high physiological stress and decreased sink activity. Conversely, a rapid decline in fluorescence yield (i.e. rapid leaf death) indicated lower physiological stress at the time of sampling (Burke 2007).

Leaf-level photosynthesis, stomatal conductance and water-use efficiency (WUE)

At the beginning (0 d) and the end (7 d) of the water-deficit stress treatment, leaf level gas exchange was measured on a recently, fully expanded, second nodal leaf during peak photosynthetic activity in midday (1000–1300 h) on peanut plants growing in the glasshouse using a portable photosynthesis system (Li-Cor model 6400, Lincoln, NE, USA). Leaves in the Li-Cor 6400 cuvette were maintained and measured under the following conditions: 38 Pa CO_2, leaf temperature 27 °C, relative humidity 50–60% and saturating photosynthetic photon flux density (PPFD) of 1900 μmol m^{-2} s^{-1} (determined by photosynthetic light response curves for three plants of each genotype) provided by a blue–red LED external light source on the Li-Cor 6400 cuvette. Leaf vapour pressure deficit (D_L) averaged 1.86 kPa for irrigated plants and 2.34 kPa for stressed plants. Estimates of instantaneous leaf WUE were calculated as the ratio of photosynthesis (A) to stomatal conductance (g_s).

Epicuticular wax estimation

Leaf discs (1.132 cm^2) were collected from 15 well-watered and 15 water-stressed plants at the end of the stress experiment. Epicuticular wax load (EWL) was estimated by both gravimetric and colorimetric methods using the protocol described by Samdur *et al.* (2003) and Ebercon, Blum & Jordan (1977).

Preparation of total crude protein extract and one-dimensional (1-D) gel electrophoresis (1-DGE)

Total leaf protein was extracted using the phenol extraction protocol described by Kottapalli *et al.* (2008) (Supporting Information Fig. S1). Briefly, 100 mg of lyophilized tissue, pooled from three plants, was added to an extraction medium containing 0.9 M sucrose, 0.1 M Tris–HCl (pH 8.8), 10 mM ethylenediaminetetraacetic acid (EDTA) (pH 8.0), 0.4% (v/v) 2-mercaptoethanol and tris-buffered phenol (pH 8.8), and gently mixed at room temperature (RT). Proteins were precipitated by incubating the phenolic phase with 0.1 M ammonium acetate–methanol at –20 °C overnight, followed by precipitation and washing of the proteins serially in three organic solvents to give a highly purified protein pellet. The protein content was measured by Bradford assay using bovine serum albumin (fraction V) as the standard (Bradford 1976). Fifteen micrograms of protein was incubated for 3 min at 95 °C in sample buffer containing 62 mM Tris (pH 6.8) containing 10% (v/v) glycerol, 2.5% (w/v) sodium dodecyl sulphate (SDS) and 5% (v/v) 2-mercaptoethanol, and a drop of bromophenol blue (BPB), then cooled to RT. After incubation on the bench (at ambient RT of 25 °C) for 10 min, the mixture was centrifuged and the supernatant was used for SDS–polyacrylamide gel electrophoresis (SDS–PAGE, 4% T, 2.6% C stacking gels, pH 6.8 and 12.5% T, 2.6% C separating gels, pH 8.8). SDS–PAGE was carried out on a Nihon Eido (Tokyo, Japan) vertical electrophoresis unit at constant current of 40 mA for ca. 4 h. The running buffer was composed of 0.025 M Tris, 0.192 M glycine and 0.2% (w/v) SDS. Molecular mass markers (5.0 μL of the commercially available 'ready-to-use' Precision Plus Protein Standards, Dual Color; Bio-Rad, Hercules, CA, USA) were loaded in the well adjacent to the samples. Gels stained with Coomassie brilliant blue (CBB R-250) were visualized for differential banding pattern.

Immunoblotting

Electrotransfer of proteins from a gel to a polyvinyldifluoride (PVDF) membrane (NT-31, 0.45 μM pore size; Nihon

Eido) was conducted at 1 mA cm^{-2} for 80 min at RT using a semidry blotter (Nihon Eido) as described in Rakwal *et al.* (2003). The ECL + plus Western Blotting Detection System protocol (GE Healthcare, Little Chalfont, Buckinghamshire, UK) was used for blocking, and primary and secondary antibody (anti-Rabbit IgG, horseradish peroxidase linked whole antibody; from donkey) incubation. Immunoassayed proteins were visualized on an X-ray film (X-OMAT AR, Kodak, Tokyo, Japan) using an enhanced chemiluminescence protocol (GE Healthcare).

Two-dimensional gel electrophoresis (2-DGE)

2-DGE of three selected genotypes was carried out using IPG strip gels on an IPGphor unit followed by the second dimension using ExcelGel XL SDS 12–14 gradient gels on a Multiphor II horizontal electrophoresis unit (GE Healthcare, Piscataway, NJ, USA). The volume carrying 80 μg total soluble protein was mixed with LB-TT (for details, see Kottapalli *et al.* (2008)) containing 0.5% (v/v) pH 4.0–7.0 IPG buffer (GE Healthcare) to bring to a final volume of 340 μL. A trace of BPB was added and samples were centrifuged at 15 000 *g* for 15 min followed by pipetting into an 18 cm strip holder tray placed into the IPGphor unit. The IPG strips (pH 4.0–7.0; 18 cm) were placed onto the protein samples, avoiding air bubbles between the sample and the gel. The IPG strips were passively rehydrated with the protein samples for 90 min, followed by overlaying the IPG strips with cover fluid; this was directly linked to a five-step active rehydration and focusing protocol (18 cm strip) as described previously (Hirano *et al.* 2007). The whole procedure was conducted at 20 °C, and a total of 68 902 Vh was used for the 18 cm strip. Following IEF, the IPG strips were immediately used for the second dimension or stored at –20 °C.

The strip gels were incubated twice in equilibration buffer containing 50 mM Tris–HCl (pH 8.8), 6 M urea, 30% (v/v) glycerol, 2% (w/v) SDS and 2% (w/v) dithiothreitol (DTT) for 10 min with gentle agitation, followed by incubation in the same equilibration buffer supplemented with 2.5% (w/v) iodoacetamide for 10 min at RT. For horizontal electrophoresis, 18 cm IPG strips were placed onto the SDS 12–14% gradient gels after equilibration, followed by placement of the cathode and anode buffer strips and electrodes, respectively. SDS–PAGE (20 and 40 mA/gel) was performed as per manufacturer recommendations (GE Healthcare). Molecular masses were determined by running Dual Color Precision plus Protein Standard protein markers (Bio-Rad); for each sample, a minimum of four IPG strips and corresponding SDS–PAGE was used under the same conditions.

Protein visualization, image analysis and spot quantification

To visualize the protein spots, the polyacrylamide gels were stained with CBB. Protein patterns in the gels were recorded as digitized images using a digital scanner (Canon CanoScan 8000F, resolution 300 dpi, 16-bit grayscale pixel depth) and saved in tagged image file formats. The gels were quantified in profile mode using ImageMaster 2D Platinum software version 5.0 (GE Healthcare, Little Chalfont, Buckinghamshire, UK). Protein abundance was expressed as relative volume according to the normalization method provided by ImageMaster software that compensates for gel-to-gel variation in sample loading, gel staining and destaining (Agrawal & Thelen 2005; Hajduch *et al.* 2005). In order to analyse differences in relative protein abundance, spot volumes were compared with those of corresponding spots in fully irrigated control samples; spot differences were also manually confirmed. Moreover, the CBB-stained spots were selected for comparative profiling only if they were confirmed in three independent gel replications.

Spots that exhibited ± 1.5-fold difference (in all three gel replications) in relative abundance in water-stressed plants compared to well-watered plants were selected for mass spectrometry analysis. Additionally, the protein bands from 1-D gels showing differential accumulation between samples were excised along with the corresponding bands from control sample lanes and transferred to sterile 1.5 mL tubes. Distinct differentially expressed protein spots from two-dimensional (2-D) gels were picked using a gel picker (One Touch Spot Picker, P2D1.5 and 3.0; The Gel Company, San Francisco, CA, USA); excised bands/spots were stored at –30 °C.

Protein identification using mass spectrometry

Proteins were identified using peptide mass fingerprinting (PMF) methods (Jensen *et al.* 1997) utilizing mass spectrometry. In the PMF method, excised gel spots were destained with 100 μL of destain solution (30 mM potassium ferricyanide in 100 mM sodium thiosulphate), with shaking for 5 min. After the solution was removed, gel spots were incubated with 200 mM ammonium bicarbonate (hereafter refered to as AMBIC) for 20 min. Gel pieces were dried in a speed vacuum concentrator for 5 min and then rehydrated with 20 μL of 50 mM AMBIC containing 0.2 μg modified trypsin (Promega, Madison, WI, USA) for 45 min on ice. After removal of solution, 30 μL of 50 mM AMBIC was added, and the digestion was performed overnight at 37 °C. The peptides were desalted and concentrated using C18 nanoscale (porous C18) columns (IN2GEN, Seoul, Korea). In preparation for use in the matrix-assisted laser desorption/ionization–time-of-flight mass spectrometer (MALDI–TOF MS), peptides were eluted by 0.8 μL of matrix solution (70% acetonitrile, 0.1% TFA, 10 mg mL^{-1} alpha-cyano-4-hydroxycinnamic acid) and then spotted onto a stainless steel target plate. Masses of peptides were determined using MALDI–TOF MS (model MALDI-R; Micromass, Manchester, UK); calibration was performed using internal mass of trypsin auto digestion product (m/z 2211.105).

In preparation for analysis by quadrupole time-of-flight tandem mass spectrometry (Q-TOF MS/MS), 15 μL of the

peptide solution from the digestion supernatant was diluted with 30 μL in 5% formic acid, loaded onto the column and washed with 30 μL of 5% formic acid. Peptides were eluted with 2.0 μL methanol/H_2O/formic acid (50/49/1, v/v/v) directly into a precoated borosilicate nanoelectrospray needle (EconoTip; New Objective, Inc., Woburn, MA, USA). MS/MS of peptides generated by in-gel digestion was performed by nano-ESI on a Q-TOF2 MS using a source temperature of 80 °C. A potential of 1 kV was applied to the precoated borosilicate nanoelectrospray needles in the ion source combined with a nitrogen back-pressure of 0–5 psi to produce a stable flow rate (10–30 nL min^{-1}). The Q-TOF2 MS was operated in an automatic data-dependent mode to collect ion signals from the eluted peptides. In this mode, the most abundant peptide ion peak with doubly or triply charged ion in a full-scan mass spectrum (m/z 400–1500) was selected as the precursor ion. Finally, an MS/MS spectrum was recorded to confirm the sequence of the precursor ion using collision-induced dissociation (CID) with a relative collision energy dependant on molecular weight; cone voltage was 40 V. The quadrupole analyser was used to select precursor ions for fragmentation in the hexapole collision cell. The collision gas was Ar at a pressure of $6–7 \times 10^{-5}$ mbar, and the collision energy was 20–30 V. Product ions were analysed using an orthogonal TOF analyser, fitted with a reflector, a micro-channel plate detector and a time-to-digital converter; data were processed using a MassLynx (ver. 3.5) Windows NT PC system.

Protein identification was performed by searching the National Center for Biotechnology Information (NCBI) non-redundant database using the MASCOT search engine (Matrix Science, London, UK; http://www.matrixscience.com), which uses a probability-based scoring system. The following parameters were used for database searches (NCBInr 20070120, 4462937 sequences; 1534242322 residues) with MALDI–TOF PMF data: trypsin as digesting enzyme, carbamidomethylation of cysteine as a fixed modification, oxidation of methionine as variable modification, monoisotopic mass, unrestricted protein mass, ± 100 ppm peptide mass tolerance, 1+ peptide charge state, with one missed cleavage allowed. For MALDI–TOF MS data to qualify as a positive identification, a peptide score had to equal or exceed the minimum significant score. For database searches (NCBInr 20070127, 4496228 sequences; 1544738466 residues; Taxonomy Viridiplantae, 283484 sequences) with MS/MS spectra, the following parameters were used: trypsin as digesting enzyme, carbamidomethylation of cysteine as a fixed modification; oxidation of methionine as allowable variable modifications, monoisotopic mass value and unrestricted protein mass; ± 1.0 Da peptide mass tolerance and ± 0.8 Da fragment mass tolerance; peptide charge of +1, +2 or +3; with one missed cleavage allowed. Positive identification of proteins by MS/MS analysis required a minimum of two unique peptides, with at least one peptide having a significant ion score.

Gene expression analysis using real-time qRT-PCR

Total RNA from leaf tissue was isolated using the RNeasy Plant Mini-kit (Qiagen, Valencia, CA, USA). Leaves were ground to a fine powder in liquid nitrogen, and approximately 100 mg of homogenized tissue was used for total RNA isolation. RNA samples were treated with Turbo DNAfree (Ambion, Austin, TX, USA) prior to cDNA synthesis. One microgram of total RNA was used to synthesize first-strand cDNA using the SuperScript First Strand Synthesis system for RT-PCR (Invitrogen, Carlsbad, CA, USA). The primers for eight candidate proteins identified from this study were designed using Integrated DNA Technologies primer designing tools (see Supporting Information Table S1). The efficiency of the primer pairs was determined using cDNA derived from the irrigated samples using a 1:2 serial dilution series. Primer efficiency reactions were performed in triplicate in a volume of 25 μL using SuperArray SYBRGreen reaction mix (SuperArray Bioscience Corp., Frederick, MD, USA).

Reactions were subjected to real-time qRT-PCR using the Roche LightCycler 480 Real-Time PCR System and analysed using the LightCycler 480 quantification software (Roche Biochemicals, Indianapolis, IN, USA). Samples were analysed in a 25 μL reaction volume using the Roche LightCycler. Reactions were performed in triplicate using cDNA templates from treated and control samples for each gene (candidate genes and *actin*-DF gene). A master mix of SYBRGreen and primers was prepared for each primer pair. RT-PCR reactions were performed on 40 ng total RNA with 400 nM specific primers under the following conditions: one cycle of denaturation at 95 °C for 10 min followed by 40 cycles each consisting of 95 °C for 15 s (denaturation) and 60 °C for 15 s (annealing and elongation). The PCR reaction was followed by a melting curve programme (60–95 °C with a heating rate of 0.1 °C s^{-1} and a continuous fluorescence measurement) and then a cooling programme at 40 °C. Negative controls lacking reverse transcriptase were run with all reactions. PCR products were also run on agarose gels to confirm the formation of a single product at the desired size. Crossing points for each transcript were determined using the second-derivative maximum analysis with the arithmetic baseline adjustment. Crossing point values for each gene were normalized to the respective crossing point values for the reference gene *actin*-DF. Data were presented as normalized ratios of genes along with error standard deviations estimated using the Roche Applied Science E-method (Tellmann & Geulen 2006).

Statistical analyses

Each experiment was replicated at least three times. Values are expressed as means ± SE. Data were analysed using KaleidaGraph (Synergy Software, Reading, PA, USA) software. All mean comparisons were done using *t*-test for independent samples. For photosynthetic rate and stomatal

conductance, the different measurements were subjected to a one-way analysis of variance (ANOVA). Confidence coefficient α in all cases was set at 0.05.

RESULTS AND DISCUSSION

Screening of US peanut mini-core genotypes for water-deficit stress tolerance

We evaluated 17 genotypes from the US peanut mini-core collection and three check cultivars using the chlorophyll fluorescence screening technique following imposition of water-deficit stress. Of these 20 genotypes, we identified five stress-tolerant (COC041, COC384, COC249, COC149, TMV-2) and five stress-susceptible (COC166, COC227, COC068, Tamrun OL02, ICGS 76) genotypes based on observations of chlorophyll fluorescence yield (Fig. 1a), whole-plant WUE (mg mass produced per g of water used; Fig. 1b), and specific leaf area (SLA; cm^2 leaf area per g leaf mass; Fig. 1c). Tolerant genotypes were characterized by smaller percentage changes in chlorophyll fluorescence yield during water-deficit stress, higher WUE during well-watered and deficit stress conditions and slightly higher SLA, compared with susceptible genotypes. The most tolerant genotype (COC041) exhibited a similar decline in fluorescence yield over time in both water-stressed and well-watered plants (Fig. 1d). In contrast, the most susceptible genotype (COC166) exhibited a marginal decline in fluorescence yield in the water-stressed plants after 72 h of incubation. The tolerant genotype (COC041) also exhibited higher whole plant WUE than the susceptible genotype (COC166).

Our results indicate that the elevated respiratory demand bioassay, designed to measure source leaf responses to abiotic stresses in cotton (Burke 2007), can be employed to screen peanut genotypes for divergence in response to water-deficit stress. Here, we have designated COC041 as a stress-tolerant genotype and COC166 as stress susceptible based on higher relative whole-plant WUE and normal chlorophyll fluorescence under stress conditions compared to other selected US mini-core accessions and check cultivars during water-deficit stress. As further confirmation of our designation of COC041 as a tolerant genotype and COC166 as susceptible, we compared the yield of these genotypes under field conditions of full and moderate deficit irrigation of approximately 100 and 70% potential evapotranspiration (PET) replacement, respectively. When grown in deficit irrigation conditions of 70% PET, the susceptible genotype exhibited approximately 90% decline in yield, while the tolerant genotype exhibited a 15–20% decline in yield compared to the 100% PET treatment (Fig. 2a,b).

Leaf physiological responses to water stress

Figure 3 shows that light-saturated photosynthesis (A) was similar in the tolerant (COC041) and susceptible (COC166) genotypes before water stress was applied (0 d) and at the end of the stress period (7 d), but A was higher in the susceptible genotype during stress exposure (3 d) because of higher stomatal conductance (g_s; Table 2). On the second day after rewatering, A and g_s were higher in the tolerant genotype reflecting faster recovery from stress, but 7 d after rewatering both genotypes had fully recovered (Table 2). Instantaneous leaf-level WUE (A/g_s; WUE) was higher in the tolerant genotype prior to and during the onset of water deficit because of lower g_s. However, upon return to saturated soil moisture conditions, assimilation rates and stomatal conductance increased rapidly (within 48 h), and WUE was lower in the tolerant genotype compared to the susceptible genotype. Although the susceptible genotype showed a slower recovery following the stress treatment, both genotypes recovered to pre-stress levels of photosynthesis 7 d after rewatering (Table 2). In general, the response to soil moisture availability is significantly faster in the tolerant genotype compared to susceptible plants, and this appears to be, in part, caused by better stomatal control.

Differences in protein profiles between tolerant and susceptible genotypes

1-DGE was used to identify broad protein-level differences between the tolerant and susceptible genotypes and the check cultivar. On 12.5% SDS–PAGE gels, 43 differential bands were observed in the tolerant genotype (COC041), susceptible genotype (COC166) and check cultivar (TMV2) under well-watered and water-deficit conditions (Fig. 4). Only those bands showing distinct differences between stressed and well-watered samples (23 in total) were selected for LC-MS/MS analysis, generating the identification of 17 non-redundant proteins (Table 3).

Changes in protein profiles in the susceptible, tolerant and check cultivar peanut plants during water stress were observed in 2-DGE analysis of total proteins (Fig. 5). Quantitative image analysis indicated 79 differential protein spots exhibited significantly altered intensities ($\pm$ 1.5-fold over well-watered control) in water-stressed plants. These 79 differential proteins were then analysed by MALDI–TOF MS and Q-TOF MS/MS, and 48 non-redundant proteins with altered intensities were observed ($\pm$ 1.5-fold over well-watered control) in water-stressed plants (Table 4). Spectra of all proteins identified by MALDI and Q-TOF are provided in our peanut protein database (http://www.lbk.ars.usda.gov/psgd/index-peanut.aspx).

We categorized these proteins into 10 different known functional groups (representing 83% of proteins) and one, relatively small unknown group (13% of proteins; Fig. 6). Surprisingly, the identities of very few differentially expressed proteins were unknown. This may be because of the fact that majority of abundant leaf proteins have been well characterized (Larrainzar *et al.* 2007). The largest functional groups were proteins associated with photosynthesis (25%), lectins (15%), signal transduction (13%) and water stress (10%). Apart from the known enzymes involved in photosynthesis, five proteins implicated in signal

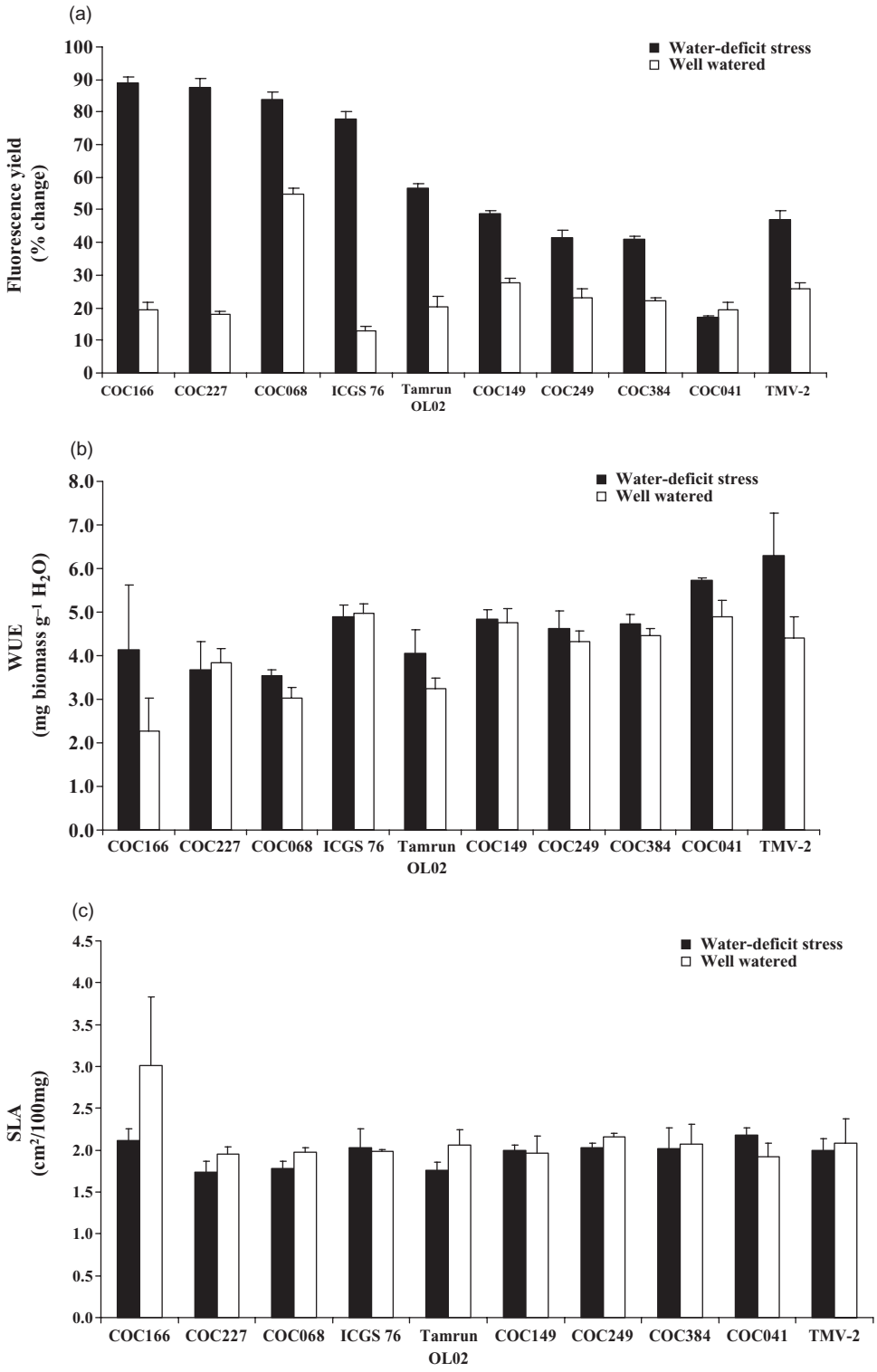

Figure 1. (a) Percent change in chlorophyll fluorescence yield for 10 selected peanut genotypes exposed to slow-onset water-deficit stress for 7 d. The chlorophyll fluorescence values indicate the percent change in yield at 72 h compared to 0 h. (b) Water-use efficiency (WUE) calculated as the ratio of biomass produced per given amount of water (mg g^{-1}). (c) Specific leaf area (SLA) given as ratio of leaf area and leaf dry mass (cm^2 100 mg). (d) Graphs showing time-course chlorophyll fluorescence yield decline of control (white squares) and water-stressed (black squares) source leaves of peanut genotypes COC041 and COC166, and cultivar TMV2.

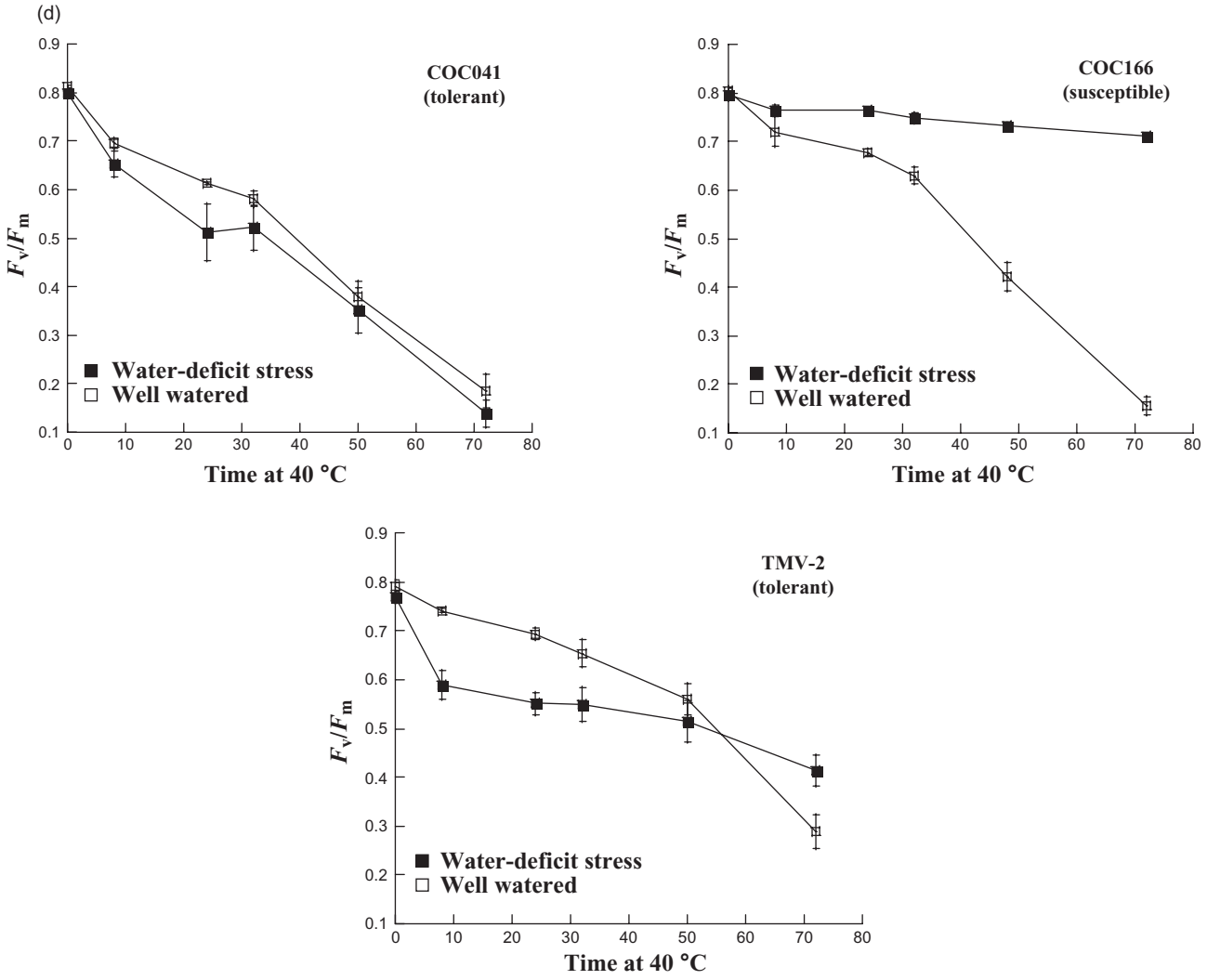

Figure 1. *Continued.*

transduction were detected during water stress (Tables 3 and 4). These included lipoxygenase (LOX) (Table 3, band 5), cyclophilin (Table 3, band 14), calmodulin-binding protein (CBP) (Table 3, band 15), nucleoside diphosphate kinase 1 (NDK1) (Table 3, band 16) and 1L-myo-inositol-1-phosphate synthase (Table 4, spot 30). Levels of LOX protein increased during water stress in tolerant genotypes. Fatty acid hydroperoxide-like linolenic acid produced by LOX is a precursor for biosynthesis of jasmonic acid, a signalling molecule that activates plant defence mechanisms (Lee *et al.* 2005). It is possible that jasmonic acid, produced by lipoxygenase, may be involved in perception and transduction of extracellular signals during water stress. However, it should be noted that the role of LOX in the stress response is complex (Fauconnier *et al.* 2002), and the possible involvement of jasmonic acid, here, requires further investigation. On the other hand, the increase in 1L-myo-inositol-1-phosphate synthase during stress suggests its indirect involvement in water stress signalling through phosphoinositoids. 1L-Myo-inositol-1-phosphate synthase catalyses the reaction from glucose-6-phosphate to inositol-1-phosphate [I(1)P], the first step of myo-inositol biosynthesis. Phosphoinositides synthesized from I(1)P are plasma membrane-bound proteins and involved in signal transduction (Yoshida *et al.* 1999).

Previous studies showed that nucleoside diphosphate kinases (NDKs) play a role in GTP-mediated signal transduction pathways, light response and reactive oxygen scavenging, and are involved in plant response to heat and water deficit (Pan *et al.* 2000; Galvis *et al.* 2001; Fukamatsu, Yabe & Hasunuma 2003; reviewed by Hasunuma *et al.* 2003; Hajheidari *et al.* 2005; Bhushan *et al.* 2007). NDK1 protein was highly induced under water-deficit stress in sweet potato (Hajheidari *et al.* 2005), but its expression was reduced in a stress-tolerant chickpea cultivar grown under water-deficit stress (Bhushan *et al.* 2007). Interestingly, in our study, levels of NDK1 protein increased only in the susceptible genotype in response to water-deficit stress (Table 3, band 16). Contrastingly, NDK1 levels decreased in response to water deficit in the

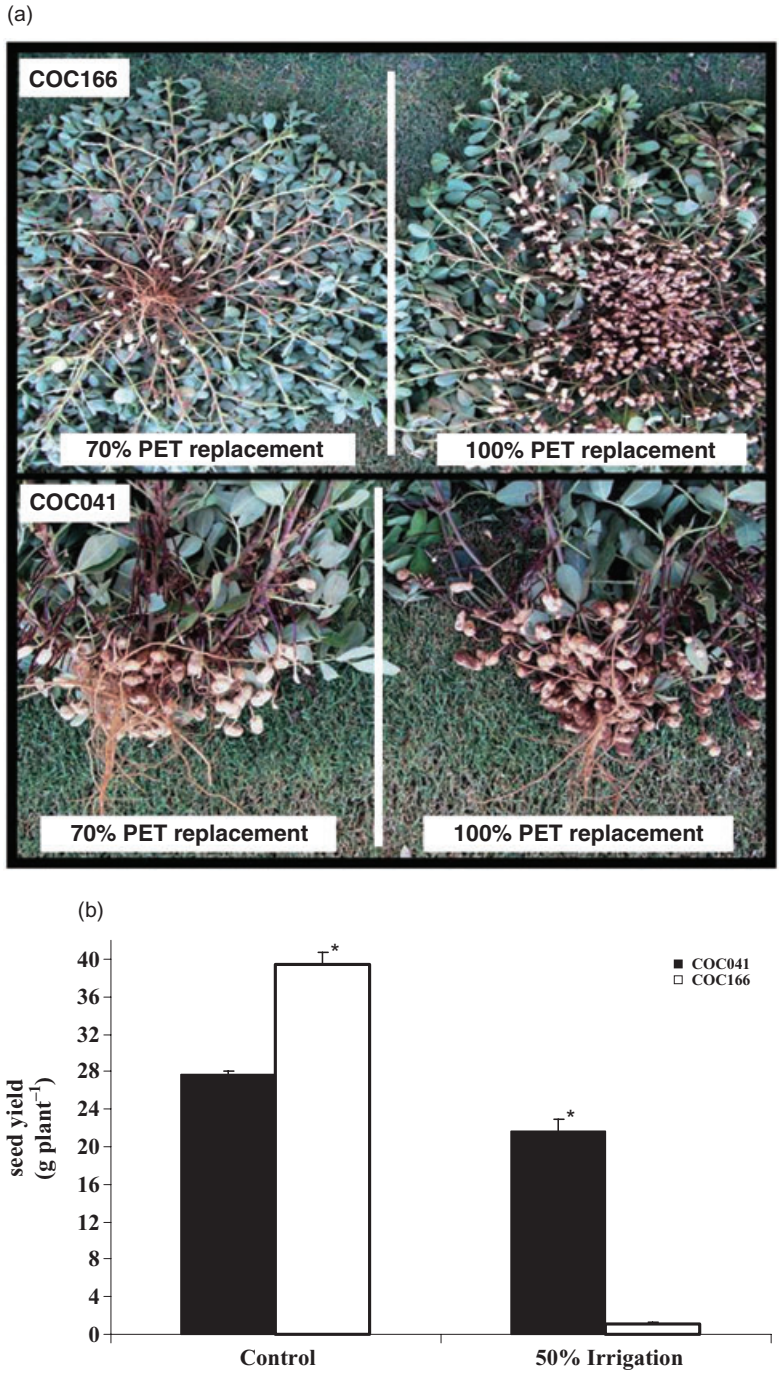

Figure 2. (a) Comparison of pod yield for COC166 (top panel) and COC041 (bottom panel) grown under deficit irrigation [70% potential evapotranspiration (PET) replacement] in 2008 field trials conducted at the ARS Cropping Systems Laboratory in Lubbock, TX, USA. (b) Under moderate water-deficit conditions, COC166 shows approximately 90% decrease in pod yield, while COC041 shows roughly a 22% decrease in yield compared to fully irrigated plants. Statistically significant differences were measured for all comparisons, and those were $P < 0.001$ are indicated as *.

tolerant cultivar TMV2 and could not be detected in the tolerant COC041 genotype plants. Whether this indicates that COC041 leaves were not under the same level of water-deficit stress experienced by TMV2 and COC166 or an alternative mechnism or absence of this protein in COC041 is unknown. However, transcript for this gene was induced in all three genotypes in response to water-deficit stress.

The cyclophilin protein was induced both in the susceptible genotype and the TMV2 cultivar, and remained

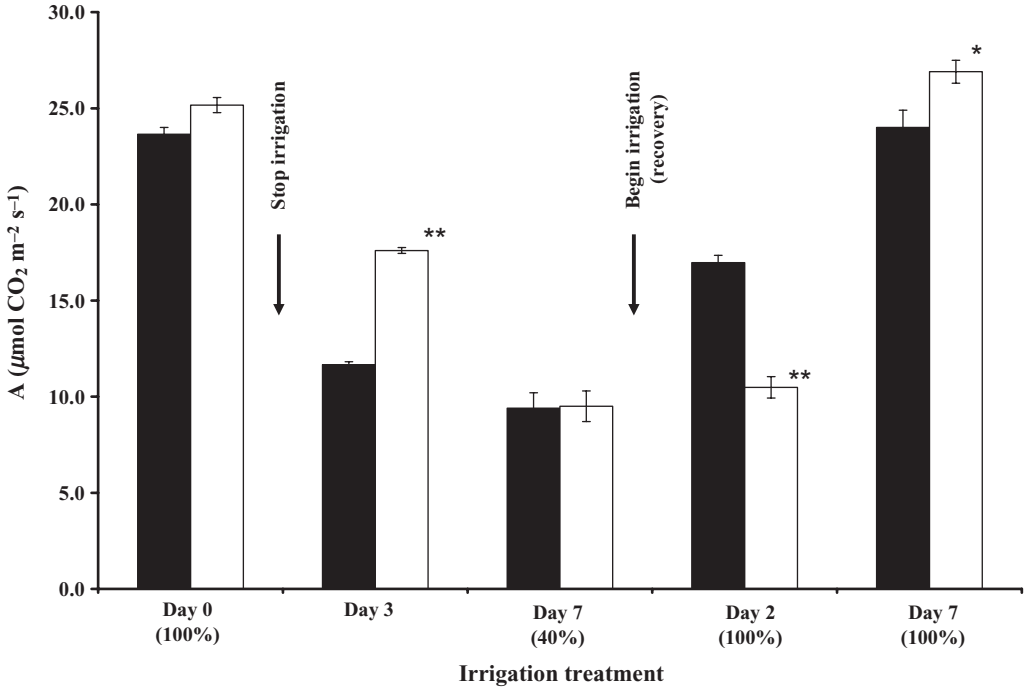

Figure 3. Photosynthetic response to water-deficit stress in COC041 (black bars) and COC166 (white bars). Data are mean values of net photosynthesis ± SEs ($n \geq 6$ for each measurement). Statistically significant differences are indicated as $^{**}P \leq 0.01$ and $^{*}P \leq 0.05$.

unchanged in the tolerant COC041. Cyclophilins differentially expressed during water stress are involved in a variety of cellular processes. Besides protein folding function, they also play a role in signal transduction and thus may be crucial for stress responsiveness (Romano, Horton & Gray 2004). In sugarbeet and sorghum, cyclophilins were accumulated in the tolerant cultivars during water-deficit stress (Hajheidari *et al.* 2005). However, in chickpea, the cyclophilin-like peptidyl-prolyl *cis-trans* isomerase was reduced during dehydration in the tolerant cultivar (Bhushan *et al.* 2007). Our work with peanuts and that of Bhushan *et al.* (2007) with chickpeas suggest negative signalling of cyclophilins in these two legume species. Another signalling protein, calmodulin, is a ubiquitous calcium receptor that regulates the activities and functions of a wide range of CBPs. A significant increase in the protein was seen in the susceptible genotype and may be involved in forming complexes with CBP like GAD or protein kinases (Fromm & Snedden 1997) required for calcium signalling in response to water-deficit stress. Absence of induction of the

Table 2. Stomatal conductance (g_s; mol H_2O m^{-2} s^{-1}), transpiration (E; mmol H_2O m^{-2} s^{-1}) and estimates of water-use efficiency (WUE) (A/g_s and A/E) for COC041 and COC166 plants exposed to slow-onset water-deficit stress for 7 d followed by rewatering to soil saturation daily for 7 d

	g_s		E		A/g_s		A/E	
	COC041	COC166	COC041	COC166	COC041	COC166	COC041	COC166
Water deficit								
Day 0	0.412	0.478	6.28	9.58	52.9	40.8**	4.4	2.1*
	(0.026)	(0.08)	(1.02)	(1.29)	(9)	(1.8)	(1)	(0.1)
Day 3	0.102	0.142	3.39	4.69*	115.4	112.9*	3.4	3.4
	(0.007)	(0.018)	(0.2)	(0.53)	(5.3)	(5.3)	(0.2)	(0.2)
Day 7	0.063	0.069	1.78	2.04	152.8	139.8**	5.7	5.1
	(0.007)	(0.009)	(0.17)	(0.25)	(4.7)	(4.9)	(0.5)	(0.8)
Rewater								
Day 2	0.316	0.188**	7.78	4.61**	52.1	88.2**	2	2.9*
	(0.06)	(0.101)	(0.62)	(0.15)	(4.4)	(5)	(0.2)	(0.2)
Day 7	0.458	0.655***	9.4	11.72***	54.2	42.8*	2.6	2.3
	(0.046)	(0.04)	(0.59)	(0.41)	(4.2)	(2.1)	(0.1)	(0.1)

Data are mean values with SEs in parentheses ($n \geq 6$).
Statistically significant differences are indicated at $^{***}P \leq 0.001$, $^{**}P \leq 0.01$ and $^{*}P \leq 0.05$.

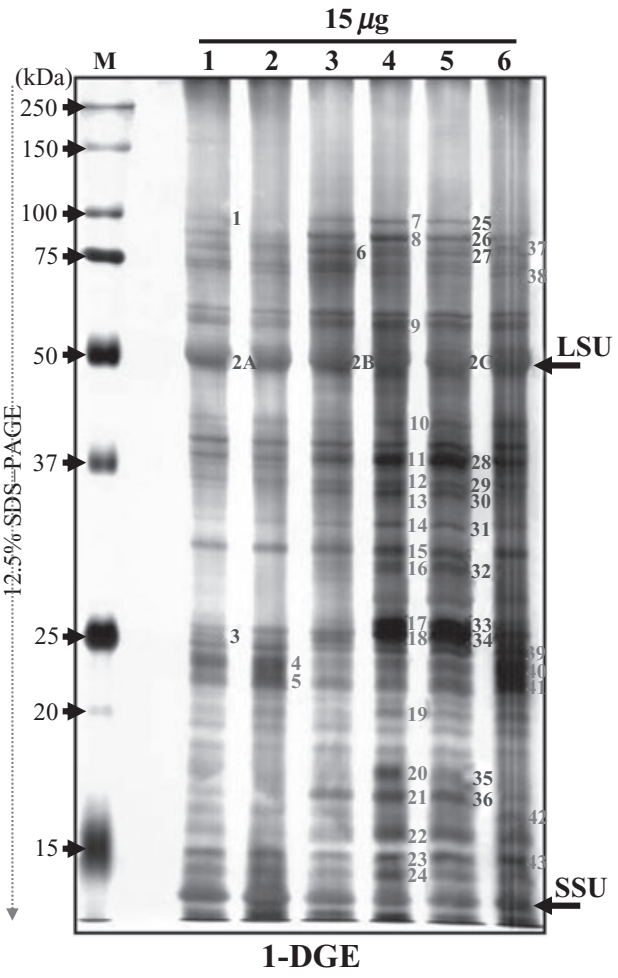

Figure 4. Coomassie brilliant blue (CBB)-stained one-dimensional (1-D) gel protein profiles of leaves from control and water-stressed plants (equal protein amounts ca. 15 μg were applied) was carried out as described in Materials and methods. Leaf proteins from COC041 control (1), COC041 water stress treated (2), COC166 control (3), COC166 water stress treated (4), TMV2 control (5), TMV2 water stress treated (6) were mentioned above each lane. Molecular weights (kDa) of protein markers (Precision Plus Protein Standards) are indicated at the left. Sodium dodecyl sulphate–polyacrylamide gel electrophoresis (SDS–PAGE) (4% T, 2.6% C stacking gels, pH 6.8 and 12.5% T, 2.6% C separating gels, pH 8.8) was carried out using 12.5% polyacrylamide gels on a Nihon Eido (Tokyo, Japan) vertical electrophoresis unit at constant current of 40 mA for ca. 4.5 h. The running buffer was composed of 0.025 M Tris, 0.192 M glycine and 0.2% (w/v) SDS. Five microlitres of the commercially available 'ready-to-use' molecular mass standards (Precision Plus Protein Standards, Dual Color) was loaded in the well adjacent to the samples.

protein in tolerant genotype COC041 suggests that either the plants are not experiencing the same level of stress or a possible mechanism to avoid stress by blocking the transmission of signals to CBP.

Interestingly, a tetratricopeptide repeat containing protein (TPR) (Table 4, spot 78), a positive regulator of ABA signalling during plant development under stress was induced in the tolerant line and check cultivar with the latter showing more specific induction of the protein (Fig. 5). The TPR-containing proteins were shown to be stress responsive in soybean under heat stress (Torres, Chatellard & Stutz 1995) and *Arabidopsis* in response to salt and osmotic stress (Rosado *et al.* 2006). The *Arabidopsis* TPR-containing *TTL1* mutants have reduced tolerance to salt and osmotic stress, characterized by reduced root elongation and disorganization of the root meristem. It was also shown that *TTL1* regulates the transcript levels of several dehydration-responsive genes including the transcription factor DREB2A (Rosado *et al.* 2006). Further, it was demonstrated that *TTL1* acts as a positive regulator of ABA signalling during plant development under stress. Thus, TPR-containing proteins may function as members of multiprotein complexes implicated in the regulation of ABA signalling and abiotic stress responses in the tolerant peanut genotype.

Our proteomics analysis also identified proteins involved in ameliorating water stress. Methionine synthase (Table 4, spot 1), the enzyme responsible for synthesis of *S*-adenosyl methionine (SAM), was reduced in all three genotypes during water deficit. Lignification of the cell wall by methylation of lignin monomers may be one mechanism to avoid water loss under dehydration (Bhushan *et al.* 2007). Additionally, changes in phenylpropanoid biosynthesis, namely methylation of lignin precursors by *S*-adenosyl methionine synthetase and the production of ferulic acid represent key steps in cell wall lignification and cell expansion (Chazen and Neumann 1994; Neuman 1995; Riccardi *et al.* 1998). In this reaction, SAM serves as the primary methyl group donor. Cellular levels of SAM are regulated by the activity of methionine synthase which generates methionine, a precursor of SAM (Ravanel *et al.* 1998, 2004). Induction of methionine synthase transcript suggests an increased production of methionine and lignin methylation by SAM. On the other hand, reduction of the protein under water stress in all accessions may be caused by a demand for more methyl groups for lignin methylation.

For proteins involved in photorespiration, we detected glycine dehydrogenase (decarboxylating) (Table 3, band 17), which was induced in the susceptible genotype during water stress. The glycine dehydrogenase enzyme family consists of glycine cleavage system P-proteins EC 1.4.4.2 from bacterial, mammalian and plant sources. The P protein is part of the glycine decarboxylase (GDC; EC 2.1.2.10) multienzyme complex, and catalyses the interconversion of glycine to serine, an integral part of the photorespiratory pathway (Bauwe & Kolukisaoglu 2003). It has been suggested that decreased GDC in pea mitochondria following exposure to water-deficit stress is a result of oxidative damage and that GDC inhibition may serve as an initial marker of oxidative stress in plant cells (Taylor, Day & Millar 2002). Reduction of this protein in TMV2 may indicate damage to the photorespiratory pathway during water-deficit stress, while increased expression of GDC in susceptible plants suggests the possible involvement of photorespiration as an electron sink in minimizing reactive

Table 3. Peanut leaf protein identification by tandem mass spectrometry (MS) from silver nitrate-stained protein bands visuliazed on one-dimensional gel electrophoresis (1-DGE)

Band No.	Treatment	Protein identified	Relative abundance	Score	Sequence coverage	Accession	Peptide
1	Control	Type III chlorophyll *a/b*-binding protein	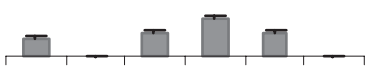	48	5	gi|20794	YAMLGAVGAIAPEILGK
	Control	Carbonic anhydrase, chloroplast precursor (Carbonate dehydratase) **EC 4.2.1.1**		47	5	gi|115472	EAVNVSLGNLLTYPFVR
	WS	Oxygen-evolving enhancer protein 2, chloroplast precursor (OEE2)		76	8	gi|131390	SITDYGSPEEFLSKVDYLLGK
	WS	Carbonic anhydrase, chloroplast precursor (Carbonate dehydratase) **EC 4.2.1.1**		60	5	gi|115472	EAVNVSLGNLLTYPFVR
2A	Control	Ribulose-1·5-biphosphate carboxylase-oxygenaselarge subunit		309	–	gi|2342884	@
	WS	ATP synthase beta subunit **EC 3.6.3.14**		391	–	gi|16943747	@
2B	Control	ATP synthase beta subunit		219	–	gi|14717962	
	WS	ATP synthase beta subunit **EC 3.6.3.14**		172	–	gi|7708286	@
	WS	Ribulose-1·5-biphosphate carboxylase-oxygenaselarge subunit		188	–	gi|17066183	@
2C	Control	ATP synthase beta subunit		179	–	gi|5001575	@
	Control	Ribulose-1·5-biphosphate carboxylase-oxygenaselarge subunit		172	–	gi|2342884	@
	WS	ATP synthase beta subunit **EC 3.6.3.14**		285	–	gi|66276267	@
	WS	Ribulose-1·5-biphosphate carboxylase-oxygenaselarge subunit		268	–	gi|1770291	@
3	Control	Carbonic anhydrase, chloroplast precursor (Carbonate dehydratase)		31	5	gi|115472	EAVNVSLGNLLTYPFVR
	Control	751(+2) – MS/MS, permease protein of sugar ABC transporter		66	90**	Q98JY6	EYNLLPDHLVG***
	WS	Carbonic anhydrase, chloroplast precursor (Carbonate dehydratase) **EC 4.2.1.1**		53	5	gi|115472	EAVNVSLGNLLTYPFVR
	WS	Unknown		ND	ND	ND	ALSPHVLDWRALVMAMR*
4	Control	Heat shock protein 81-1 (HSP81-1) (Heat shock protein 82)		42	2	gi|417154	GIVDSEDLPLNISR
	WS	Unknown		ND	ND	ND	LTTSLDGVTAYNAL
5	Control	Phospholipase D		22	1	gi|1698844	LEGPIAWDVLFNFEQR
	WS	Lipoxygenase **EC 1.13.12.11**		30	2	gi|439857	YGPAKMPYTLLYPSSEEGLTFR
	WS	1125(+2) – MS/MS, Seed lipoxygenase-1 (**EC 1.13.11.12**) (L-1)		88	91**	P08170	KPNEDYPYAADGLELADGALK***

Table 3. *Continued*

Band No.	Treatment	Protein identified	Relative abundance 1 2 3 4 5 6	Score	Sequence coverage	Accession	Peptide
6	Control	Glyceraldehyde-3-phosphate dehydrogenase, cytosolic	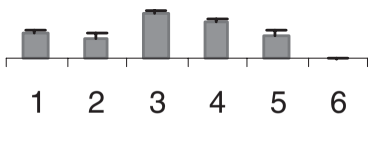	84	8	gi|120666	AASFNIIPSSTGAAK, LVSWYDNEWGYSTR
	Control	Aldolase		70	12	gi|169039	TVVSIPNGPSALAVK, YAAISQDNGLVPIVEPEILLDGEH GIDR
	WS	Glyceraldehyde-3-phophate dehydrogenase, cytosolic **EC 1.2.1.12**		135	10	gi|120666	GILGYTEDDVVSTDFVGDSR, LVSWYDNEWGYSTR
7	Control	918(+2) – MS/MS, Anti-H(O) lectin I (CSA-I)	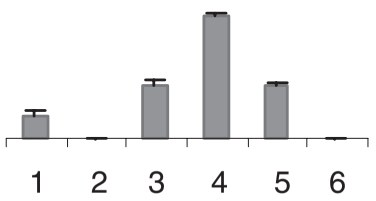	25	91**	P22970	ELQDGLTFFLAPALSSK***
	WS	918(+2) – MS/MS, Anti-H(O) lectin I (CSA-I)		57	76**	P22970	QNAGDGLTFMLAPAS***
8	Control	Oxygen-evolving enhancer protein 1, chloroplast precursor (OEE1)	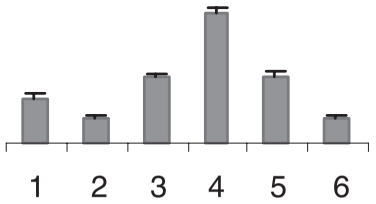	69	9	gi|11134054	ITLSVTQSKPETGEVIG VFESIQPSDTDLGAK
	Control	810(+3) – MS/MS, 36 kDa outer mitochondrial membrane protein (porin)		66	90**	P42056	SSNENTLTLGYAN***
	WS	1132(+2) – MS/MS, same as control, Unknown					
10	Control	Chlorophyll *a*/*b*-binding protein of LHCII type I, chloroplast precursor (CAB) (LHCP)	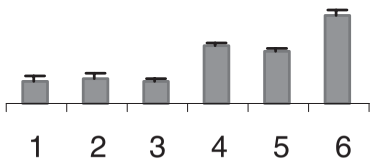	44	13	gi|115768	IAGGPLGEVTDPIYPGGS FDPLGLADDPEAFAELK
	Control	870(+2) – MS/MS, Chlorophyll *a*/*b*-binding protein		63	80**	ABE80774	ATPFQPYSEVFVAQR***
	WS	870(+2) – MS/MS, Chlorophyll *a*/*b*-binding protein**					
	WS	729(+2) – MS/MS, Lectin precursor		60	80**	Q5ZEW9	VLAVEMDTFFDR***
	WS	897(+2) – MS/MS, Mannose/ glucose-binding lectin precursor (Fragment)		62	69**	Q43376	SCHSLNVLVTYDGSSR***

11	Control	Major Cab protein		80	27	gi|169193	PGGSFDPLGLADDPEAFAELK
	Control	Chlorophyll *a*/*b*-binding protein of LHCII type I, chloroplast precursor (CAB) (LHCP)		68	13	gi|115768	IAGGPLGEVTDPIYPGGS FDPLGLADDPEAFAELK
	WS	LHCII type I chlorophyll *a*/*b*-binding protein		97	19	gi|9587207	WAMLGALGSVFPELLAR, IAGGPLGEVTDPIYPGGSFD PLGLADDPEAFAELK
12	Control	Failed					
	WS	Cytoplasmic ribosomal protein L18		68	5	gi|606970	APLGQNTVLLR
	WS	Peptide 751 *m*/*z* – Permease protein of sugar ABC				Q98JY6	WTAAASYALALATSPK**
	WS	811(+2) – MS/MS, Unknown					LTPDYDALDVANKLGLL**
13	Control	916(+2) – MS/MS, 60S ribosomal protein L23a (L25)					
	WS	60S ribosomal protein L23a (L25)		39	11	gi|585876	LTPDYDALDVANKIGII
	WS	698(+2) – MS/MS					NGGLYMLLGTLG**
14	Control	Cyclophilin		59	6	gi|939726	VVMELFADVTPR
	WS	Ribosomal protein L12		112	19	gi|3986695	VTGGEVGAASSLAPK, VSVVPSAAALVIK
	WS	Cyclophilin		56	6	gi|939726	VVMELFADVTPR
	WS	Cyclophilin		53	8	gi|829119	VFFDMTIGGQPAGR
	WS	Histone H2B.1		45	9	gi|12202	AMSIMNSFINDIFEK
15	Control	792(+2) – MS/MS, Calmodulin-binding protein 60-A (Fragment)		76	76**	Q8H6U0	ELVANEDMQHLLR***
	Control	842(+2) – MS/MS					NTVDDGSPLLLSSPLR***
	WS	60S ribosomal protein L23a (L25)		62	11	gi|585876	LTPDYDALDVANKIGII
	WS	792(+2) – MS/MS, Calmodulin-binding protein 60-A (Fragment)					ELVANEDFQHLLR***
16	Control	887(+2) – MS/MS, Nucleoside diphosphate kinase I (**EC 2.7.4.6**) (NDK I)		50	62**	P47922	QNQTFLMLQ***
	WS	Peptide 887 *m*/*z*					

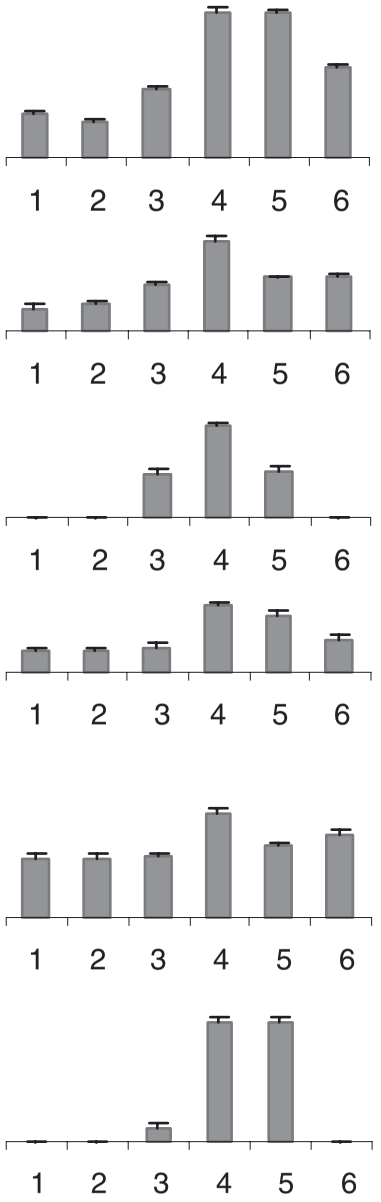

Table 3. *Continued*

Band No.	Treatment	Protein identified	Relative abundance 1 2 3 4 5 6	Score	Sequence coverage	Accession	Peptide
17	Control	Lipoxygenase (EC 1.13.11.12) 3 – soybean	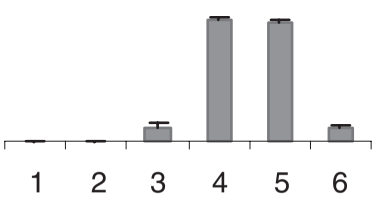	74	2	gi|81793	LVIEDYPYAVDGLEIWDAIK
	WS	1122(+2) – MS/MS, Glycine dehydrogenase [decarboxylating], mitochondrial precursor (**EC 1.4.4.2**)		67	90**	P26969	FDETTSLEDVHAVTPV***
22	Control	751(+2) – MS/MS, Permease protein of sugar ABC transporter*	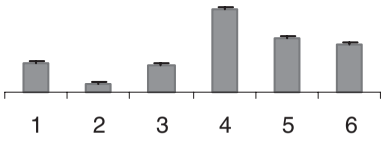	66	90**	Q98JY6	EYNLLPDHLVG***
	WS	Ribulose-phosphate 3-epimerase, chloroplast precursor (Pentose-5-phosphate 3-epimerase) (PPE) (RPE) (P5P3E)		54	5	gi|2499728	SDIIVSPSILSANFSK
	WS	646(+2) – MS/MS, Chlorophyll *a*/*b*-binding protein type III (Fragment)		74	72**	Q9M538	WLAYGELLDGR***
	WS	729(+2) – MS/MS, Carbonic anhydrase					NVANLVPPAALNHE***
23	Control	Cyclophilin	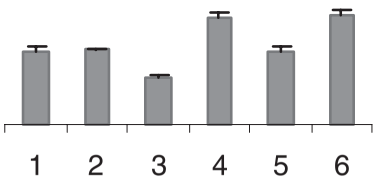	57	6	gi|939726	VVMELFADVTPR
	WS	Cyclophilin		38	6	gi|939726	VVMELFADVTPR

Relative abundance of selected proteins is shown as a bar graph: lane 1, COC041 well watered; lane 2, COC041 water stressed; lane 3, COC166 well watered; lane 4, COC166 water stressed; lane 5, TMV2 well watered; lane 6, TMV2 water stressed.
WS, water stress; @, proteins identified by one-dimensional (1-D) shotgun of the excised band resulting in multiple hits, but score and accession number of the first hit for each protein were mentioned in the table, and peptide sequences of all hits are provided in Supporting Information Table S2.
*, estimated sequence; **, protein identity; ***, *de novo* sequence.
Differences between the treatments were significant at $P < 0.0001$.

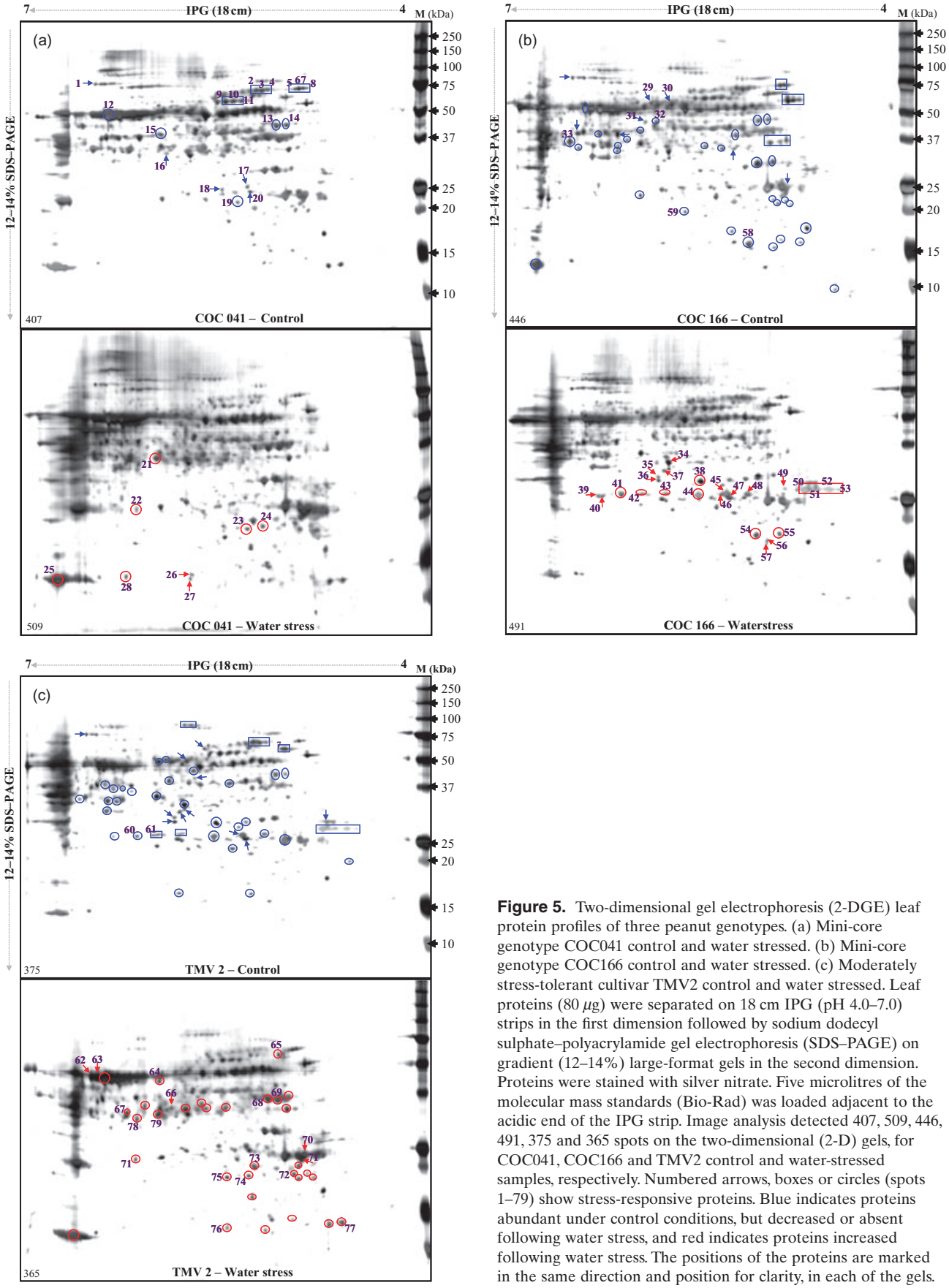

Figure 5. Two-dimensional gel electrophoresis (2-DGE) leaf protein profiles of three peanut genotypes. (a) Mini-core genotype COC041 control and water stressed. (b) Mini-core genotype COC166 control and water stressed. (c) Moderately stress-tolerant cultivar TMV2 control and water stressed. Leaf proteins (80 μg) were separated on 18 cm IPG (pH 4.0–7.0) strips in the first dimension followed by sodium dodecyl sulphate–polyacrylamide gel electrophoresis (SDS–PAGE) on gradient (12–14%) large-format gels in the second dimension. Proteins were stained with silver nitrate. Five microlitres of the molecular mass standards (Bio-Rad) was loaded adjacent to the acidic end of the IPG strip. Image analysis detected 407, 509, 446, 491, 375 and 365 spots on the two-dimensional (2-D) gels, for COC041, COC166 and TMV2 control and water-stressed samples, respectively. Numbered arrows, boxes or circles (spots 1–79) show stress-responsive proteins. Blue indicates proteins abundant under control conditions, but decreased or absent following water stress, and red indicates proteins increased following water stress. The positions of the proteins are marked in the same direction and position for clarity, in each of the gels.

oxygen production induced by water-deficit stress (Osmond & Grace 1995; Kozaki & Takeba 1996; Noctor *et al.* 2002).

Acetyl CoA carboxylase (ACC) mediated cell wall strengthening under water stress

Interestingly, ACC (Table 4, spots 26 and 27), which is an enzyme involved in lipid biosynthesis, was uniquely identified in the tolerant genotype (COC041) and detectable only during water stress. In plants, ACC isozymes provide the malonyl CoA pools used for *de novo* fatty acid synthesis in plastids and mitochondria, and for fatty acid elongation, flavonoid (FL) and stilbene biosynthesis in the cytosol (Focke *et al.* 2003). From several studies, it is evident that the ACC reaction is the most important regulatory step, controlling metabolite flow in response to stress. From the water-deficit stress tolerance perspective, fatty acids are essential in membrane biogenesis, lipoic acid and cuticular wax synthesis and stress signalling (Zuther *et al.* 2004). Under extreme water deficit when stomata are nearly completely closed, water loss is primarily through cuticular transpiration (Shepherd & Griffiths 2006). In response to water stress, epicuticular wax deposition is initiated within a few days (Premachandra *et al.* 1991), and tolerant plants often have thicker leaf wax than susceptible plants (Shepherd & Griffiths 2006). To test this hypothesis, we measured the EWL in both well-watered and water-stressed plants. Interestingly, there was significantly higher EWL in the tolerant genotype (COC041) compared to the susceptible genotype (COC166) under normal conditons. Although EWL was slightly increased in the tolerant genotype during stress, there was a significant decrease in EWL in the susceptible genotype (COC166) (Fig. 7). In alfalfa, transgenic plants with increased cuticular waxes showed reduced water loss and decreased chlorophyll leaching, thereby enhancing tolerance to water-deficit stress (Zhang *et al.* 2005). These results support our hypothesis that a higher level of ACC protein in tolerant peanut leaves leads to increased amounts of polyunsaturated fatty acids, thicker cuticular wax and flavonoids for water-deficit stress signalling.

Reduction in photosynthesis-related proteins during water stress in tolerant genotypes

Nine differentially accumulated protein spots (Table 4, spots 12, 13, 14, 23, 34, 62, 63, 68, 74) were identified as Rubisco large subunit (LSU) or small subunit (SSU). 1-DGE and Western blot with Rubisco LSU indicated a general reduction in Rubisco protein content in both tolerant (COC041) and susceptible (COC166) genotypes (Fig. 4). However, the protein was increased in the moderately tolerant cultivar (TMV2) during water stress. 2-D analysis revealed five spots (12, 13, 14, 68, 74) identified as fractions of Rubisco protein that were also reduced in the leaves of the tolerant genotypes (COC041 and TMV2). Carbonic anhydrase (CA) (Table 3, bands 1 and 3) and oxygen evolving enhancer protein 2 (OEP) of photosystem II (PSII) were also reduced in the tolerant genotype (COC041). Interestingly, another nuclear-encoded PSII protein, psbP (Table 4, spot 73), decreased only in the tolerant genotype. The abundance of two protein bands identified as photosynthesis-related chlorophyll *a*/*b*-binding protein (Table 3, bands 11 and 22) also declined in the tolerant genotype, but its homolog (Table 4, spot 71) was induced during water-deficit stress. Together, these results suggest an overall reduction of photosynthesis-related proteins during water stress in the tolerant peanut genotypes. Correlated with this decrease in major photosynthetic proteins was a rapid decrease in transpiration and photosythetic rate in the tolerant genotype compared to susceptible plants (Table 2; Fig. 3).

Increased ATP synthase and ferredoxin–NADP reductase to meet energy demand during water stress

Because water stress substantially decreases CO_2 assimilation by net reduction in the amount of ATP (Tezara *et al.* 1999), it was suggested that induction of ATP synthesis will assist in abiotic stress tolerance (Zhang, Liu & Takano 2008). In the current study, an ATP synthase epsilon chain (Table 4, spot 28) and an ATP synthase beta subunit (Table 3, band 2A) were highly induced only in tolerant genotypes suggesting their putative role in water-stress tolerance. ATP synthase plays a central role in energy transduction in chloroplasts and mitochondria, and alleviation of stress. The protein was reported to be induced in salt-stressed rice leaves (Kim *et al.* 2005) and shoots and roots of maize (Zörb *et al.* 2004). Over-expression of the ATP synthase gene resulted in greater tolerance to drought in *Arabidopsis* (Zhang *et al.* 2008). Induction of the protein in tolerant peanut genotypes may alleviate water-deficit stress by increasing ATP supply to meet increased stress-related energy demand. In addition, ferredoxin–NADP reductase which is involved in electron transfer, was also induced in all the genotypes and may help in meeting the energy demand during stress.

Lectin and lactoglutathione lyase proteins as water-deficit stress markers

Several lectins including galactose-binding and mannose/glucose-binding isoforms (bands 7, 10, and spots 17, 18, 36, 38–50, 60 and 61) were highly induced in the susceptible genotype. By contrast, lectin proteins remained either unchanged or undetectable in the tolerant COC041 and TMV2 genotypes. While the role of lectins in the plant stress response is not clear, several studies have shown induction of specific lectins in response to both abiotic and biotic stresses, and provided some evidence for lectins in diverse functions from cell wall modification to regulation of gene expression (Van Damme *et al.* 2004; Bhushan *et al.* 2007; Aghaei *et al.* 2008; Jia *et al.* 2008). Bhushan *et al.* (2007) reported induction of a mannose lectin (gi6822274) in stress-tolerant chickpea only during water-deficit stress.

Table 4. List of water stress-responsive leaf protein spots from two-dimensional gel electrophoresis (2-DGE) identified by mass spectrometry (MS)

Spot No.	Protein identified	Relative abundance	Accession	MW/pI	Score	Sequence coverage	MS	Peptide
1	Methionine synthase [*Glycine max*] **EC 1.16.1.8**	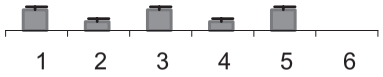	gi|33325957	84401/5.93	103	4	Q-TOF	YGWTGGEIGFDTYFSMAR/TLTSLNGVTAY GFDLVR
2	HSP70-3 (same spots = 3 and 4)	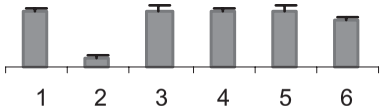	gi|15232682	71559/4.97	90	23	MALDI	TTPSYVAFTDSER/EFSAEEISSMILIKMR/NA VVTVPAYFNDSQR/DAGVIAGLNVMR/DAG VIAGLNVMR/IINEPTAAAIAYGLDK/IINEPT AAAIAYGLDKK/MVNHFVQEFKR/FEELNID LFR/DNNLLGKFELSGIPPAPR/FELSGIPPAPR /NALENYAYNMR/MYQGGEAGGPAAGGMD EDVPPSAGGAGPK
5	Heat shock protein 70 precursor [*Citrullus lanatus*] (same spots = 6–8)	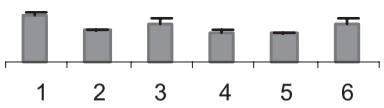	gi|1928991	75656/5.70	78	20	MALDI	QFAAEEISAQVLR/QFAAEEISAQVLRK/AVV TVPAYFNDSQR/IINEPTAASLAYGFEK/IINEP TAASLAYGFEKK/AKMELSSLTQANISLPFIT ATADGPK/FEELCSDLLYR/FEELCSDLLYRL K/DVHEVVLVGGSTRIPAVQELVK/SEVFSTA ADGQTSVEINVLQGER/SLGSFRLDGIPPAPR
12	Ribulose 1·5-bisphosphate carboxylase-oxygenase large subunit [*Dalembertia populifolia*]	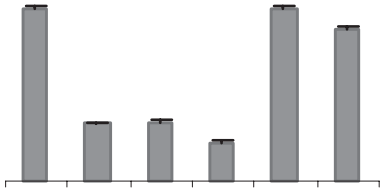	gi|62861135	51862/6.30	249	43	MALDI	LTYYTPEYETK/LTYYTPEYETKDTDILAAFR /DTDILAAFR/ALRLEDLR/LEDLRIPISYIK/IPI SYIKTFQGPPHGIQVER/TFQGPPHGIQVER/Y GRPLLGCTIKPK/GGLDFTKDDENVNSQPFM R/GGLDFTKDDENVNSQPFMR/DRFLFCAEA IFK/FLFCAEAIFK/GHYLNATAGTCEEMIKR/ DNGLLLHIHR/QKNHGMHFR/QKNHGMHFR/ LSGGDHIHAGTVVGK/LEGERDITLGFVDLL R/DITLGFVDLLR/DITLGFVDLLRDDFIEK/V ALEACVQAR/WSPELAAACEVWK/AIKFEFP AMDTL/AIKFEFPAMDTL
13	Chloroplast ribulose 1·5-bisphosphate carboxylase/ oxygenase activase small protein isoform [*Acer rubrum*]	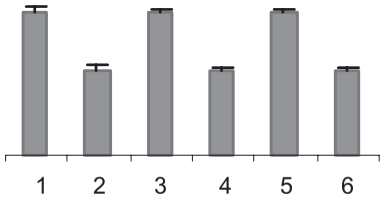	gi|115334979	47952/7.57	75	31	MALDI	NFMSLPNIKIPLILGIWGGK/SFQCELVFAK/M GITPIMMSAGELESGNAGEPAKLIR/MCCLFI NDLDAGAGR/MCCLFINDLDAGAGR/FYWA PTR/FYWAPTREDR/LVDTFPGQSIDFFGALR/ LLEYGNMLVQEQENVK/LLEYGNMLVQEQ ENVKR/VQLADKYLSEAALGDANDDAIK
14	Chloroplast ribulose 1·5-bisphosphate carboxylase/ oxygenase activase small protein isoform [*Acer rubrum*]	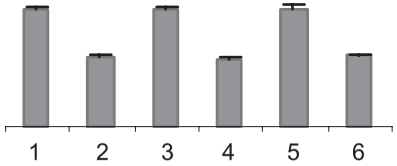	gi|115334979	47952/7.57	58	15	MALDI	SFQCELVFAK/MCCLFINDLDAGAGR/MCC LFINDLDAGAGR/FYWAPTREDR/LVDTFPG QSIDFFGALR/LLEYGNMLVQEQENVKR

Table 4. *Continued*

Spot No.	Protein identified	Relative abundance	Accession	MW/pI	Score	Sequence coverage	MS	Peptide
16	Ferredoxin–NADP reductase, leaf isozyme, chloroplast precursor (FNR) **EC 1.18.1.2**	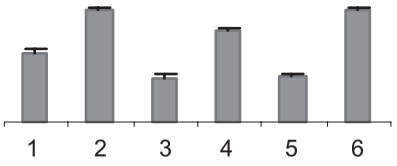	gi|119905	40454/8.56	54	4	Q-TOF	LYSIASSAIGDFGDSK
17	Lectin (same spots = 18 and 44–48)	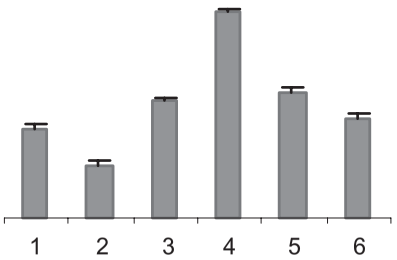	P93536		E*	E*	Q-TOF	NLLLQGDAHLDPNVLQLTR/VLAVEMDTF MDR/LQGDAHLDPNDPQLTR
21	Aldolase (same spots = 33 and 79) **EC 4.1.2.13**	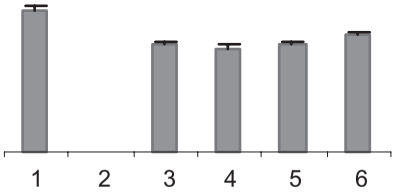	gi|169039	37974/5.47	62	8	Q-TOF	YAAISQDNGLVPIVEPEILLDGEHGIDR
23	Ribulose 1·5-bisphosphate carboxylase/oxygenase large subunit [*Forchhammeria pallida*]	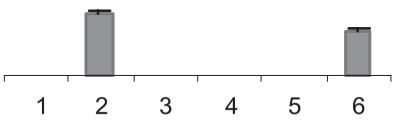	gi|46325921	38676/6.68	77	17	MALDI	LTYYTPEYETKDTDILAAFR/DTDILAAFR/ ALRLEDLR/TFQGPPHGIQVER/AVRLSGGD HVHAGTVVGK
25	Cristal-Glass1 protein [*Capsicum annuum*]	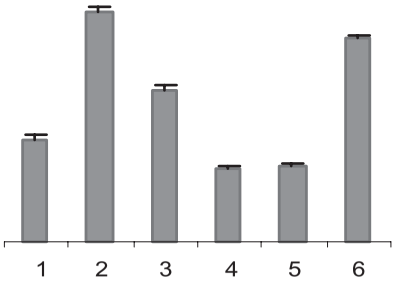	gi|40287530	20607/6.82	74	32	MALDI	SPGYYDGR/SPGYYDGRYWTMWK/YWTMW K/LPMFGCTDATQVLNEVQEAK/LPMFGCTD ATQVLNEVQEAK/LPMFGCTDATQVLNEVQ EAKK/IIGFDNVR/QVQCISFIAYKPEGY
26	Acetyl-CoA carboxylase carboxyltransferase beta subunit [*Eucalyptus globulus* subsp. *globulus*] (same spot = 27) **EC 6.4.1.2**	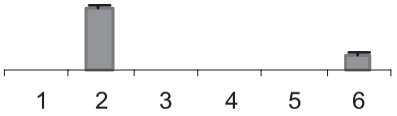	gi|108802652	56042/5.60	71	10	MALDI	MEKWWFNSMLYK/WWFNSMLYKGK/NFI SDDTFLVR/KTGLTDAVQTGTGR/GLFDPIV PRNPLK

28	ATP synthase epsilon chain (ATP synthase F1 sector epsilon subunit) **EC 3.6.3.14**	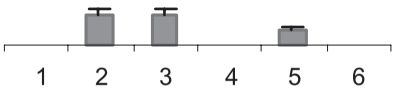	gi|114598	14654/5.84	48	12	Q-TOF	LNDQWVTMALMGGFAR
30	1L-myo-inositol-1-phosphate synthase [*Phaseolus vulgaris*] **EC 5.5.1.4**	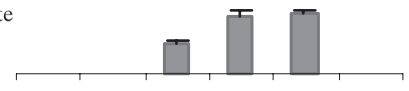	gi|14582467	52435/5.44	37	2	Q-TOF	VGSYQGEEIYAPFK
34	Ribulose 1·5-bisphosphate carboxylase/oxygenase small subunit [*Aegilops tauschii*]	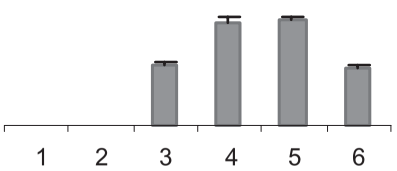	gi|4038711	18770/8.83	79	42	MALDI	VMASSATTVAPFQGLK/VMASSATTVAPFQ GLKSTAGLPVSR/IRCMQVWPIEGIK/FETLS YLPPLSTEALLK/WVPCLEFSKVGIVFR
35	Putative lactoylglutathione lyase (Methylglyoxalase) (Aldoketomutase) (Glyoxalase I) (Glx I) (Ketone-aldehyde mutase) **EC 4.4.1.5**	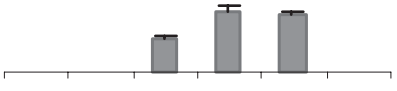	gi|2494843	31740/5.19	103	8	Q-TOF	DPDGYTFELIQR/IVSFLDPDGWK
36	Galactose-binding lectin precursor [*Arachis hypogaea*] (same spot = 38)	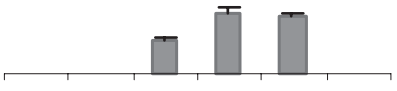	AAA74571		26.6	71**	Q-TOF	NGDLTTLADVVELK
37	Retrotransposon protein, putative, unclassified [*Oryza sativa* (japonica cultivar-group)]	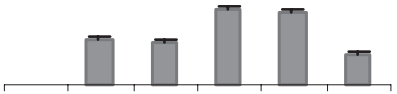	gi|77553936	84060/6.10	69	14	MALDI	AEVEPVNVIPVALEELDEGAR/AYTQDLLM KACAR/MMVPKNPEVGVWK/SNAGTSSSQA AGLTRPSGR/FNELRPLPTKMWR/HKSIEIEE PVVVQK/STKNDISETIEDFDEVEK
39	Chain A, crystal structure of dioclea violacea seed lectin (same spots = 40–43, 60 and 61)		2GDF_A		27.3	66*	Q-TOF	TSDLGDPNYPHLGLDYF
47	Flavanone 3-hydroxylase [*Citrus sinensis*] **EC 1.14.11.9**	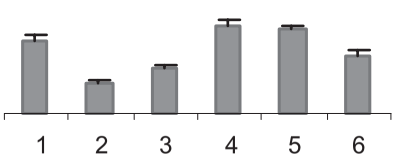	gi|4126401	40815/5.99	69	36	MALDI	MAPSTLTALAGEKTLNPSFVR/APSTLTALA GEK/TLNPSFVRFQDERPK/VAYNEFSNEIPV ISLAGIDDVGGKR/LISDMTRLATEFFALPPE EK/GGFIVSSHLQGEVVK/WPDKPEGWMEV TKEYSDK/HTDPGTITLLLQDQVGGLQATK DNGK

Table 4. *Continued*

Spot No.	Protein identified	Relative abundance	Accession	MW/pI	Score	Sequence coverage	MS	Peptide
49	Mannose/glucose-binding lectin precursor [*Arachis hypogaea*]	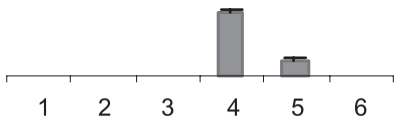	gi|951118	28372/5.36	57	10	Q-TOF	LDSLSFSYNNFEQDDERNLILQGDAK
50	Mannose/glucose-binding lectin precursor [*Arachis hypogaea*] (same spots = 51 and 52)	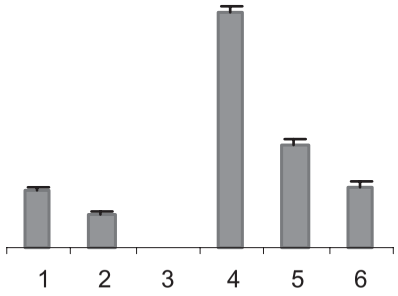	gi|951110	30994/5.71	73	8	Q-TOF	SPIDNGADGIAFFIAAPDSEIPK
62	Ribulose 1·5-bisphosphate carboxylase-oxygenase large subunit [*Arachis hypogaea*]	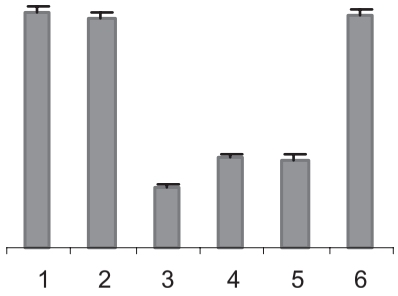	gi|2342884	51949/6.19	208	40	MALDI	LTYYTPEYETK/LTYYTPEYETKDTDILAAF R/DTDILAAFR/ALRLEDLR/LEDLRIPISYIK/ TFQGPPHGIQVER/TFQGPPHGIQVERDK/Y GRPLLGCTIKPK/AVYECLR/GGLDFTKDDE NVNSQPFMR/GGLDFTKDDENVNSQPFMR/ DRFLFCAEAIFK/GHYLNATAGTCEEMIKR/ DNGLLLHIHR/QKNHGMHFR/LSGGDHIHA GTVVGK/VALEACVQAR/EGNEIIREASK/EA SKWSPELAAACEVWK/WSPELAAACEVWK
63	Ribulose 1·5-bisphosphate carboxylase-oxygenase large subunit [*Arachis hypogaea*]	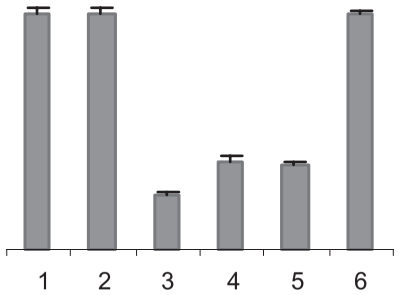	gi|2342884	51949/6.19	178	36	MALDI	LTYYTPEYETKDTDILAAFR/DTDILAAFR/A LRLEDLR/LEDLRIPISYIK/TFQGPPHGIQVE R/TFQGPPHGIQVERDK/YGRPLLGCTIKPK/ YGRPLLGCTIKPK/AVYECLR/GGLDFTKDD ENVNSQPFMR/GGLDFTKDDENVNSQPFMR /DNGLLLHIHR/QKNHGMHFR/LSGGDHIHA GTVVGK/VALEACVQAR/EGNEIIREASK/EA SKWSPELAAACEVWK/WSPELAAACEVWK /AIKFEFPAMDTL/AIKFEFPAMDTL
67	Plastidic aldolase NPALDP1 [*Nicotiana paniculata*]	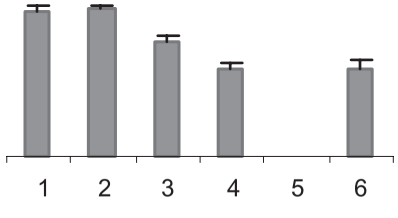	gi|4827251	42832/6.92	79	26	MALDI	GILAMDESNATCGKR/GILAMDESNATCGK R/RLASIGLENTEANR/LASIGLENTEANR/L ASIGLENTEANRQAYR/VDKGLVPLAGSND ESWCQGLDGLASR/GLVPLAGSNDESWCQG LDGLASR/SAAYYQQGAR/WRTVVSIPNGPS ALAVK/TWGGRPENVQAAQEALLIR

68	Ribulose-bisphosphate carboxylase activase (**EC 6.3.4**.-) A long form precursor – barley (fragment) (same spot = 69)	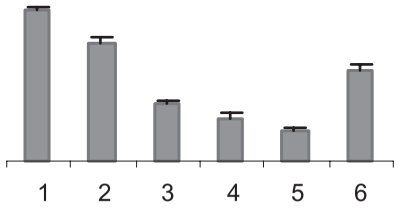	gil100614	47496/5.64	25	3	Q-TOF	IVDTFPGQSIDFFGALR
71	Putative chlorophyll *a*/*b*-binding protein [*Fagus sylvatica*]	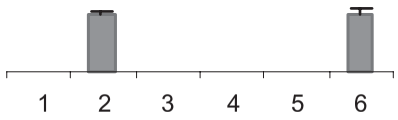	gil73665920	27685/5.14	65	12	MALDI	NVSSGSPWYGPDR/NVSSGSPWYGPDRVK/N RELEVIHSR/FGEAVWFK
73	*PsbP* [*Xerophyta humilis*]	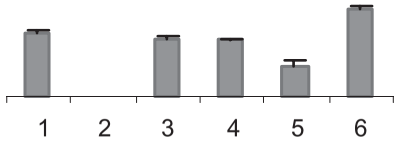	gil25992740	26347/6.84	63	5	Q-TOF	TNTDFLTYAGDGFK
74	Ribulose 1·5-biphosphate carboxylasel/oxygenase large subunit	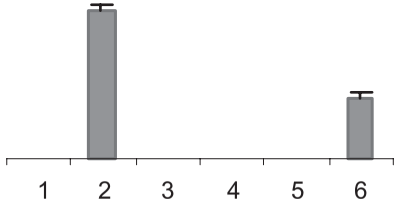	ABM63291		28.5	100**	Q-TOF	LTYYTPEYETK
78	FOG: TPR repeat (ISS) [*Ostreococcus tauri*]	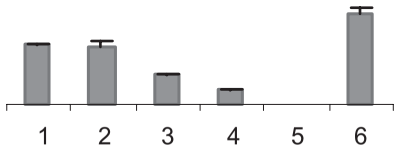	gil116000496	72518/5.09	68	10	MALDI	NAGMPSGEIAAFTKK/YQKAQ ELALR/ALASDPSDETVR/YSD LVNAIKSEFGIEK/MDLRTALT NFAAVAER

Relative abundance of selected proteins is shown as a bar graph: lane 1, COC041 well watered; lane 2, COC041 water stressed; lane 3, COC166 well watered; lane 4, COC166 water stressed; lane 5, TMV2 well watered; lane 6, TMV2 water stressed.
*, estimated sequence; **, protein identity.
Differences between the treatments were significant at $P < 0.0001$.
MALDI, matrix-assisted laser desorption/ionization; Q-TOF, quadrupole time-of-flight.

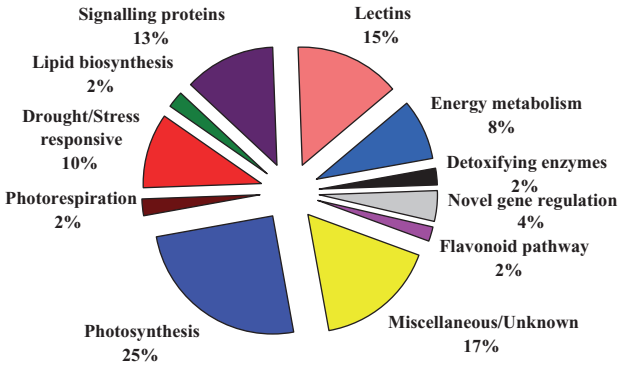

Figure 6. Functional categorization of proteins detected from both one-dimensional (1-D) and two-dimensional (2-D) gels and identified by tandem mass spectrometry (MS/MS), matrix-assisted laser desorption/ionization (MALDI) and quadrupole time-of-flight (Q-TOF) analyses.

Interestingly, lectin expression appears to be unaffected in the tolerant genotypes (COC041 and TMV2), while induced in the susceptible COC166 plants in response to water-deficit stress. Aghaei *et al.* (2008) reported a similar down-regulation of lectins in response to salt stress in soybean hypocotyls and roots. Immunoblotting studies with a rice polyclonal anti-SalT antibody revealed that the salt and water stress-inducible mannose lectin protein SalT (Claes *et al.* 1990; Kim *et al.* 2005) was also induced in the susceptible COC166 plants during stress (Fig. 8). However, in tolerant genotypes (COC041 and TMV2), the SalT protein disappeared after stress. A greater induction of lectins in COC166 could indicate that this genotype experienced severe water stress. On the contrary, tolerant genotypes might not have experienced water stress because of the presence of other compensatory mechanisms; therefore, increased abundance of SalT was not evident under water-deficit conditions. There was also a significant induction of lactoglutathione lyase (Table 4, spot 35), the protein involved in glyoxalase system, in the susceptible COC166 plants in response to water deficit, while the protein was undetectable in the tolerant genotypes. Lactoglutathione lyase is one of the two enzymes of the glyoxalase system associated with detoxification of cytotoxic methylglyoxal, formed as a by-product of carbohydrate and lipid metabolism (Thornalley 1993). The absence of this protein in the tolerant genotype (COC041) and induction in susceptible accession, as well as the contrasting amount of detectable lectins, indirectly points to the general status of cells in stress-tolerant and susceptible genotypes during water-deficit stress.

Histone H2B and retrotransposon-based novel gene regulation under water-deficit stress

A histone H2B protein was induced in the susceptible line, and the retrotransposon protein (Table 4, spot 37) appeared in the tolerant genotype (COC041) during water stress. In yeast, it was shown that histone H2B, upon ubiquitination, regulates histone H3 methylation and transcriptional silencing (Sun & Allis 2002). Such unique gene regulation mediated through '*trans*-tail' histone modification cannot be ruled out during water stress in peanuts. However, the exact mechanism of water-deficit stress tolerance involving reduction of histone proteins in the TMV2 cultivar remains enigmatic. It is known that retrotransposons can generate small RNAs (siRNA) which in turn may silence a specific gene (Watanabe *et al.* 2006). Currently, we do not know if the identified retrotransposon in tolerant peanut genotypes generates siRNA, which can knock down a gene whose product is detrimental to the cells during water stress.

Transcript response to water-deficit stress

To investigate whether changes in gene expression were correlated to changes in protein abundance, a qRT-PCR experiment was conducted using the available EST sequences of eight candidate proteins (Fig. 9). Not surprisingly, these results showed that in most instances, the

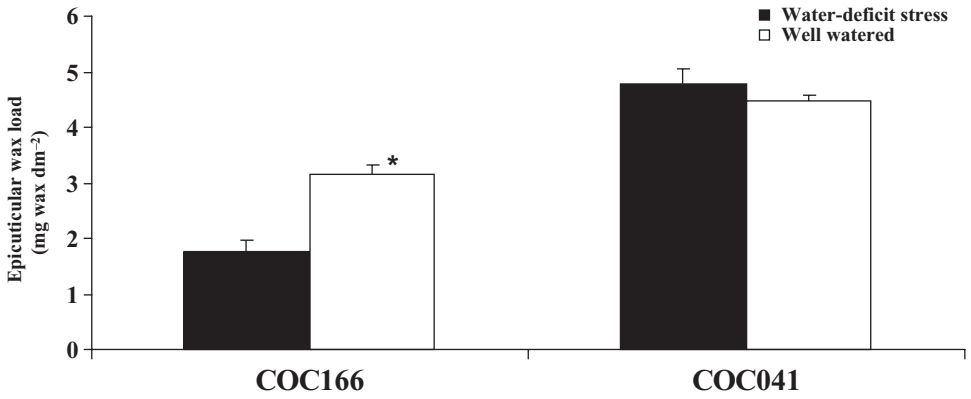

Figure 7. Leaf epicuticular wax load (EWL) of susceptible (COC166) and tolerant (COC041) peanut genotypes for water-deficit stressed leaves (black bars) 7 d post-irrigation and well-watered control plants (white bars). Bars represent mean values ± SE. Statistically significant differences are indicated as $*P = 0.0006$.

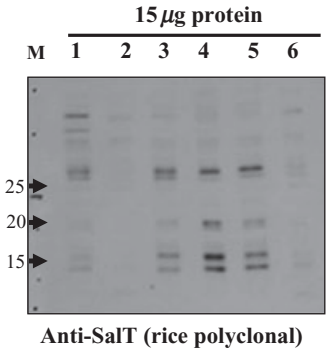

Figure 8. One-dimensional (1-D) immunoblotting showing cross-reacting SalT protein in peanut leaves. Leaves from control and water-stressed plants were sampled at 7 d post-treatment. Protein samples from COC041 control (1), COC041 water stress treated (2), COC166 control (3), COC166 water stress treated (4), TMV2 control (5), TMV2 water stress treated (6) were mentioned above each lane. Molecular weights (kDa) of protein markers (Precision Plus Protein Standards, Bio-Rad) are indicated at the left. Immunoassaying was carried out as described in Materials and methods.

mRNA levels did not correlate with protein abundance. Methionine synthase protein levels declined in all genotypes in response to water-deficit stress and were correlated with a decrease in transcript levels in TMV2 and COC166 (Fig. 9). However, the transcript for this gene nearly doubled in stressed COC041 leaves. Lectin mRNA in tolerant COC041 and methionine synthase, and TPR transcripts in TMV2 correlated with respective protein patterns. In the susceptible genotype (COC166), four transcripts (i.e. methionine synthase, NDK1, 1L-myo-inositol-1-phosphate synthase and TPR expression patterns) were well correlated with protein patterns. Several studies reported similar findings regarding changes at the transcript level which do not correlate with changes in total protein because of post-translational regulation of gene expression (Hirano *et al.* 2007; Joosen *et al.* 2007; Kottapalli *et al.* 2007b).

Theoretical model of water stress tolerance in peanuts

Based upon our results, we developed a theoretical model representing water stress tolerance in peanuts (Fig. 10). Peanut, an oilseed crop, might be utilizing its ability to adjust the lipid composition in addition to increased production of downstream metabolites (e.g. jasmonates) to reduce the impact of water stress. Initially, the perception of water stress apparently induced the production of signalling proteins, including CBP, cyclophilin, NDK1 and aldolases. Subsequently, leaves modified cell walls through lignification and wax deposition to minimize water loss. Malonyl CoA pools may also generate jasmonates through the action of lipoxygenases, which participate in long-distance signalling. Defence-related proteins (e.g. lectins and redox proteins) may be induced at a later stage. Finally, as a consequence of water stress, the photosynthetic machinery may be reversibly and partially de-activated to reduce detrimental loss of water, but may be rapidly activated upon

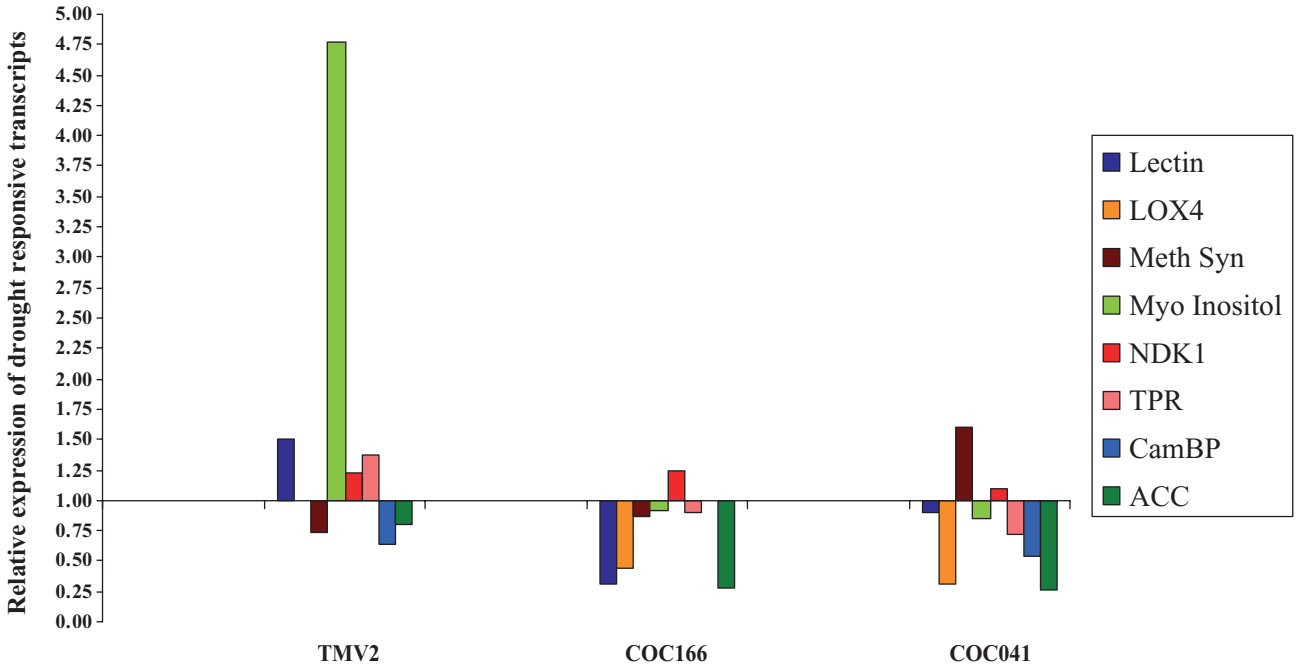

Figure 9. Real-time qRT-PCR analysis using gene-specific primers for lectin, LOX, methionine synthase, myo-inositol 1-phosphate, NDK1 and TPR. The transcript level is represented as the ratio of relative gene expressions for each cultivar (ratio of water-stressed and well-watered control). Relative quantification of gene expression was estimated by Roche E method by first normalizing the target gene to the reference actin gene followed by normalization using the calibrator (COC166 untreated) ratios.

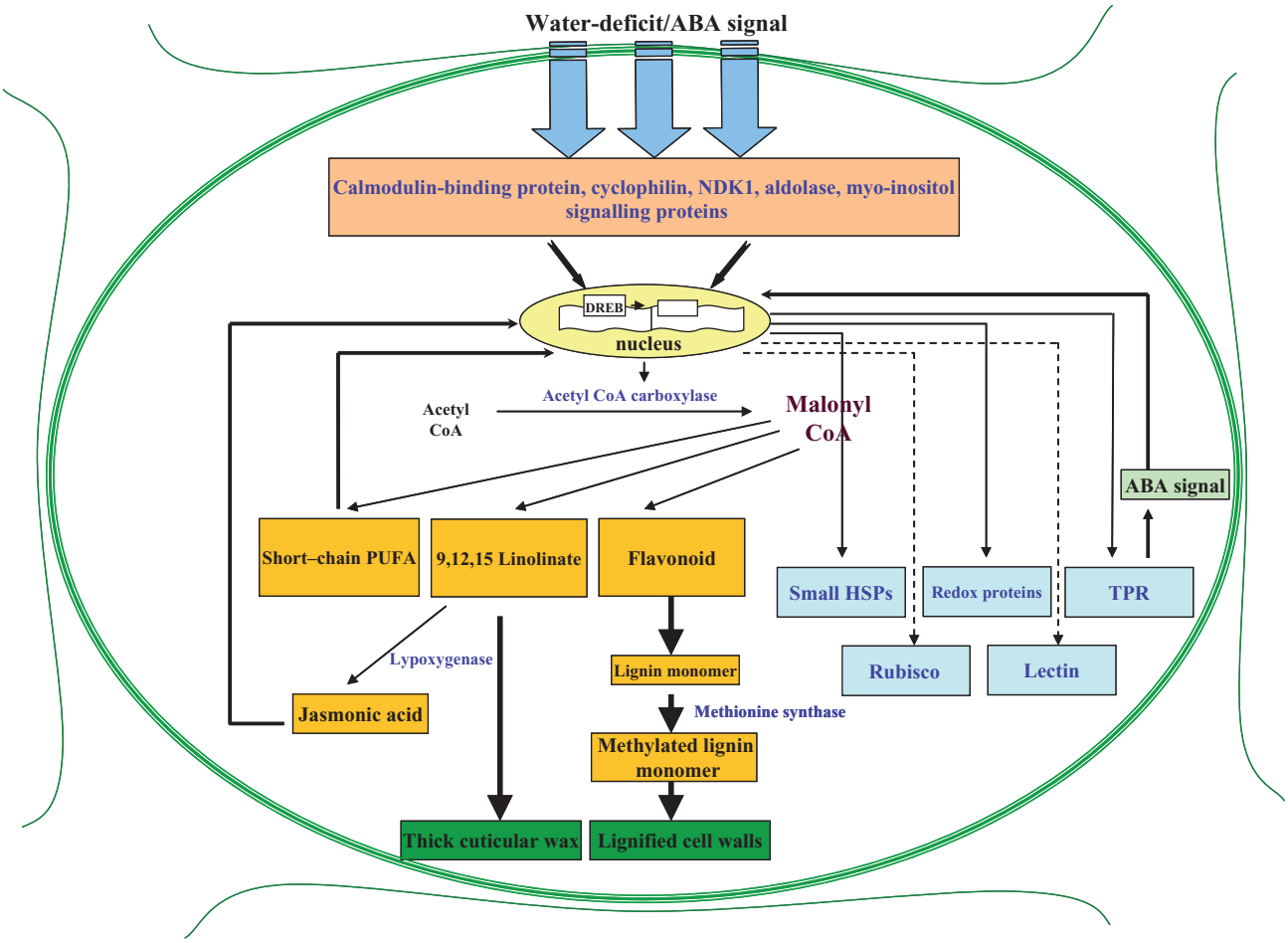

Figure 10. Representative model depicting the pathways implicated in water-deficit tolerance in peanut leaves. Proteins identified in this study are coloured in blue and displayed on the corresponding metabolic pathways. Solid arrows indicate induction of a particular protein, and dashed lines represent reduction. Dark, thick arrows show the signal molecules generated downstream of a pathway. ABA, abscisic acid; NDK1, nucleoside diphosphate kinase 1; TPR, tetratricopeptide repeat; DREB, water-deficit stress response element-binding protein.

rewatering. This is an essential trait for production agriculture where plants are continually exposed to intermittent irrigation events in both rain-fed and irrigated conditions. In our tolerant genotype (COC041), a 30% decrease in irrigation levels in the field only reduced yield by 15–20% compared with 90% in the susceptible genotype, which is a substantial difference in real-world application. This yield response appears to be correlated with a rapid down-regulation of photosynthesis via stomatal closure and decrease in photosynthetic machinery which could minimize water loss from the plant and prevent cellular damage. Additionally, higher epicuticular wax may minimize additional water loss from the tolerant genotype. Upon re-irrigation, the tolerant genotype rapidly regains a significant percentage of its non-stressed photosynthetic capacity. Interestingly, the tolerant genotypes fail to exhibit up-regulation of many proteins known to be responsive to stress, suggesting that under the similar levels of available soil moisture, the tolerant genotype does not experience the same level of stress as experienced by the susceptible genotype. Although both tolerant and susceptible plants recover full photosynthetic capacity within 1 week of re-irrigation, it is perhaps the recovery phase and potential energy costs associated with cellular repair that ultimately have an impact on significantly reducing yield in the susceptible genotype. Elucidation of the physiological mechanisms controlling these contrasting responses will be the focus of our future efforts, as well as the functional characterization of candidate genes and proteins identified here.

ACKNOWLEDGMENTS

We thank undergraduate students, Mr Kiyotaka Horie and Ms Takako Furusawa (School of Agriculture, Ibaraki University, Ami, Japan), for their technical help at AIST. The anti-SalT (rice polyclonal) was donated by Prof. Kyu Young Kang, Environmental Biotechnology National Core Research Center, Division of Applied Life Science (BK21 program), Gyeongsang National University, Jinju 660-701, Korea. This research was supported by

grants from the National Peanut Board, Texas Peanut Producers Board, New Mexico Peanut Research Board, New Mexico State University Agricultural Experiment Station, Ogallala Aquifer Initiative and USDA-ARS CRIS 6208-21000-012-00D.

REFERENCES

Aghaei K., Ehsanpour A.A., Shah A.H. & Komatsu S. (2008) Proteome analysis of soybean hypocotyl and root under salt stress. *Amino Acids* **36,** 91–98.

Agrawal G.K. & Thelen J.J. (2005) Development of a simplified, economical polyacrylamide gel staining protocol for phosphoproteins. *Proteomics* **5,** 4684–4688.

Anderson W.G., Holbrook C.C. & Culbreath A.K. (1996) Screening the core collection for resistance to tomato spotted wilt virus. *Peanut Science* **23,** 57–61.

Bauwe H. & Kolukisaoglu Ü. (2003) Genetic manipulation of glycine decarboxylation. *Journal of Experimental Botany* **54,** 1523–1535.

Bennett J., Salekdeh H., Liu J., Bruskiewich R., Kathiresan A., Lafitte R., Wadena L.J. & Gregorio G. (2002) Linking proteomic and genomic analyses of abiotic stress responses in rice and other cereals. In *Abstracts Plant and Animal Genome Meeting X*, p. 12.

Bhushan D., Pandey A., Choudhary M.K., Datta A., Chakraborty S. & Chakraborty N. (2007) Comparative proteomics analysis of differentially expressed proteins in chickpea extracellular matrix during dehydration stress. *Molecular & Cellular Proteomics* **6,** 1868–1884.

Bradford M.M. (1976) A rapid and sensitive method for the quantitation of microgram quantities of protein utilizing the principle of protein-dye binding. *Annals of Biochemistry* **72,** 248–254.

Branch W.D. & Kvien C.K. (1992) Peanut breeding for drought resistance. *Peanut Science* **19,** 44–46.

Bray E.A. (2002) Classification of genes differentially expressed during water-deficit stress in *Arabidopsis thaliana*: an analysis using microarray and differential expression data. *Annals of Botany* **89,** 803–811.

Burke J.J. (2007) Evaluation of source leaf responses to water-deficit stresses in cotton using a novel stress bioassay. *Plant Physiology* **143,** 108–121.

Chazen O. & Neumann P.M. (1994) Hydraulic signals from the roots and rapid cell-wall hardening in growing maize (*Zea mays* L.) leaves are primary responses to polyethylene glycol-induced water deficits. *Plant Physiology* **104,** 1385–1392.

Claes B., Dekeyser R., Villarroel R., Van den Bulcke M., Bauw G., Van Montagu M. & Caplan A. (1990) Characterization of a rice gene showing organ-specific expression in response to salt stress and drought. *Plant Cell* **2,** 19–27.

Devaiah K.M., Geetha B., Athmaram T.N. & Basha M.S. (2007) Identification of two new genes from drought tolerant peanut up-regulated in response to drought. *Plant Growth Regulator* **52,** 249–258.

Drame K.N., Clavel D., Repellin A., Passaquet C. & Zuily-Fodil Y. (2007) Water deficit induces variation in expression of stress-responsive genes in two peanut (*Arachis hypogaea* L.) cultivars with different tolerance to drought. *Plant Physiology and Biochemistry* **45,** 236–243.

Ebercon A., Blum A. & Jordan W.R. (1977) A rapid colorimetric method for epicuticular wax content of sorghum leaves. *Crop Science* **17,** 179–180.

FAOSTAT data (2007) [WWW document]. URL http://faostat.fao.org/ (accessed on 17 November 2008).

Fauconnier M.L., Rojas-Beltran J., Delcarte J., Dejaeghere F., Marlier M. & du Jardin P. (2002) Lipoxygenase pathway and membrane permeability and composition during storage of potato tubers (*Solanum tuberosum* L. cv Bintje and Desiree) in different conditions. *Plant Biology* **4,** 77–85.

Focke M., Gieringer E., Schwan S., Jänsch L., Binder S. & Braun H.P. (2003) Fatty acid biosynthesis in mitochondria of grasses: malonyl-coenzyme A is generated by a mitochondrial-localized acetyl-coenzyme A carboxylase. *Plant Physiology* **133,** 875–884.

Fromm H. & Snedden W.A. (1997) Role of Ca^{2+}/calmodulin in plant response to abiotic stresses: a review. *Acta Horticulture* **447,** 431–438.

Fukamatsu Y., Yabe N. & Hasunuma K. (2003) *Arabidopsis* NDK1 is a component of ROS signaling by interacting with three catalases. *Plant Cell Physiology* **44,** 982–989.

Galvis M., Marttila S., Hakansson G., Forsberg J. & Knorpp C. (2001) Heat stress response in pea involves interaction of mitochondrial nucleoside diphosphate kinase with a novel 86-kilodalton protein. *Plant Physiology* **126,** 69–77.

Hajduch M., Ganapathy A., Stein J.W. & Thelen J.J. (2005) A systematic proteomic study of seed filling in soybean. Establishment of high-resolution two-dimensional reference maps, expression profiles, and an interactive proteome database. *Plant Physiology* **137,** 1397–1419.

Hajheidari M., Abdollahian-Noghabi M., Heidari H.A.M., Sadeghian S.Y., Ober E.S. & Salekdeh G.H. (2005) Proteome analysis of sugar beet leaves under drought stress. *Proteomics* **5,** 950–960.

Hasunuma K., Yabe N., Yoshida Y., Ogura Y. & Hamada T. (2003) Putative functions of nucleoside diphosphate kinase in plants and fungi. *Journal of Bioenergetics and Biomembranes* **35,** 57–65.

Hirano M., Rakwal R., Kouyama N., Katayama Y., Hayashi M., Shibato J., Ogawa Y., Yoshida Y., Iwahashi H. & Masuo Y. (2007) Gel-based proteomics of unilateral irradiated striatum after gamma knife surgery. *Journal of Proteome Research* **6,** 2656–2668.

Holbrook C.C., Wilson D.M. & Matheron M.E. (1998) Source of resistance to pre-harvest aflatoxin contamination in peanut. *Proceedings of the American Peanut Research and Education Society* **30,** 54.

Holbrook C.C., Stephenson M.G. & Johnson A.W. (2000) Level and geographical distribution of resistance to *Meloidogyne arenaria* in the U.S. peanut germplasm collection. *Crop Science* **40,** 1168–1171.

Holbrook C.C. Jr, Cantonwine E., Sullivan D.G., Guo B., Wilson D.M. & Dong W. (2007) Development of peanut germplasm with improved drought tolerance. *Proceedings of the American Peanut Research and Education Society* **39,** 21.

Isleib T.G., Beute M.K., Rice P.W. & Hollowell J.E. (1995) Screening the peanut core collection for resistance to *Cylindrocladium* black rot and early leaf spot. *Proceedings of the American Peanut Research and Education Society* **27,** 25.

Jain A.K., Basha S.M. & Holbrook C.C. (2001) Identification of drought-responsive transcripts in peanut (*Arachis hypogaea* L.). *Electronic Journal of Biotechnology* **4,** 59–67.

Jensen O.N., Mortensen P., Vorm O. & Mann M. (1997) Automation of matrix-assisted laser desorption/ionization mass spectrometry using fuzzy logic feedback control. *Analytical Chemistry* **69,** 1706–1714.

Jia X.Y., Xu C.Y., Jing R.L., Li R.Z., Mao X.G., Wang J.P. & Chang X.P. (2008) Molecular cloning and characterization of wheat calreticulin (CRT) gene involved in drought-stressed responses. *Journal of Experimental Botany* **4,** 739–751.

Joosen R., Cordewener J., Supena E.D., *et al.* (2007) Combined transcriptome and proteome analysis identifies pathways and markers associated with the establishment of rapeseed

microspore-derived embryo development. *Plant Physiology* **144,** 155–172.

Kim D.W., Rakwal R., Agrawal G.K., *et al.* (2005) A hydroponic rice seedling culture model system for investigating proteome of salt stress in rice leaf. *Electrophoresis* **26,** 4521–4539.

Kottapalli K.R., Burow M.D., Burow G., Burke J. & Puppala N. (2007a) Molecular characterization of the U.S. peanut mini core collection using microsatellite markers. *Crop Science* **47,** 1718–1727.

Kottapalli K.R., Rakwal R., Satoh K., Shibato J., Kottapalli P., Iwahashi H. & Kikuchi S. (2007b) Transcriptional profiling of indica rice cultivar IET8585 (Ajaya) infected with bacterial leaf blight pathogen *Xanthomonas oryzae* pv oryzae. *Plant Physiology and Biochemistry* **45,** 834–850.

Kottapalli K.R., Payton P., Rakwal R., Agrawal G.K., Shibato J., Burow M.D. & Puppala N. (2008) Proteomic analysis of mature seed of four peanut cultivars using two-dimensional gel electrophoresis reveals distinct differential expression of storage, anti-nutritional, and allergenic proteins. *Plant Science* **175,** 321–329.

Kozaki A. & Takeba G. (1996) Photorespiration protects C_3 plants from photooxidation. *Nature* **384,** 557–560.

Larrainzar E., Wienkoop S., Weckwerth W., Ladrera R., Arrese-Igor C. & González E.M. (2007) *Medicago truncatula* root nodule proteome analysis reveals differential plant and bacteroid responses to drought stress. *Plant Physiology* **144,** 1495–1507.

Lee S.H., Ahn S.J., Im Y.J., Cho K., Chung G.C., Cho B.H. & Han O. (2005) Differential impact of low temperature on fatty acid unsaturation and lipoxygenase activity in figleaf gourd and cucumber roots. *Biochemical and Biophysical Research Communications* **330,** 1194–1198.

Luo M., Liang X.Q., Dang P., Holbrook C.C., Bausher M.G., Lee R.D. & Guo B.Z. (2005) Microarray-based screening of differentially expressed genes in peanut in response to *Aspergillus parasiticus* infection and drought stress. *Plant Science* **169,** 695–703.

Magalhaes J.V. (2006) Aluminum tolerance genes are conserved between monocots and dicots. *Proceedings of the National Academy of Sciences of the United States of America* **103,** 9749–9750.

Neuman P.M. (1995) The role of cell wall adjustment in plant resistance to water deficits. *Crop Science* **35,** 1258–1266.

Nigam S.N., Dwivedi S.L., Rao Y.L.C. & Gibbons R.W. (1991) Registration of 'ICGV 87141' peanut. *Crop Science* **31,** 1096.

Noctor G., Veljovik-Jovanoik S., Driscoll S., Novistkaya L. & Foyer C.H. (2002) Drought and oxidative load in the leaves of C_3 plants: a predominant role for photorespiration? *Annals of Botany (London)* **89,** 841–850.

Osmond C.B. & Grace S.C. (1995) Perspectives on photoinhibition and photorespiration in the field: quintessential inefficiencies of the light and dark reactions of photosynthesis. *Journal of Experimental Botany* **46,** 1351–1362.

Pan L., Kawai M., Yano A. & Uchimiya H. (2000) Nucleoside diphosphate kinase required for coleoptile elongation in rice. *Plant Physiology* **122,** 447–452.

Premachandra G.S., Saneoka H., Kanaya M. & Ogata S. (1991) Cell membrane stability and leaf surface wax content as affected by increasing water deficits in maize. *Journal of Experimental Botany* **42,** 167–171.

Rakwal R., Agrawal G.K., Kubo A., Yonekura M., Tamogami S., Saji H. & Iwahashi H. (2003) Defense/Stress responses elicited in rice seedlings exposed to the gaseous air pollutant sulfur dioxide. *Environmental and Experimental Botany* **49,** 223–235.

Ravanel S., Gakière B., Job D. & Douce R. (1998) The specific features of methionine biosynthesis and metabolism in plants. *Proceedings of the National Academy of Sciences of the United States of America* **95,** 7805–7812.

Ravanel S., Block M.A., Rippert P., Jabrin S., Curien G., Rébeillé F. & Douce R. (2004) Methionine metabolism in plants: chloroplasts are autonomous for *de novo* methionine synthesis and can import *S*-adenosylmethionine from the cytosol. *Journal of Biological Chemistry* **279,** 22548–22557.

Riccardi F., Gazeau P., de Vienne D. & Zivy M. (1998) Protein changes in response to progressive water deficit in maize. Quantitative variation and polypeptide identification. *Plant Physiology* **117,** 1253–1263.

Romano P.G., Horton P. & Gray J.E. (2004) The *Arabidopsis* cyclophilin gene family. *Plant Physiology* **134,** 1268–1282.

Rosado A., Schapire A.L., Bressan R.A., Harfouche A.L., Hasegawa P.M., Valpuesta V. & Botella M.A. (2006) The *Arabidopsis* tetratricopeptide repeat-containing protein TTL1 is required for osmotic stress responses and abscisic acid sensitivity. *Plant Physiology* **142,** 1113–1126.

Rucker K.S., Kvien C.K., Holbrook C.C. & Hook J.E. (1995) Identification of peanut genotypes with improved drought avoidance traits. *Peanut Science* **22,** 14–18.

Salekdeh G.H., Siopongco J., Wade L.J., Ghareyazie B. & Bennett J. (2002) Proteomic analysis of rice leaves during drought stress and recovery. *Proteomics* **2,** 1131–1145.

Samdur M.Y., Manivel P., Jain V.K., Chikani B.M., Gor H.K., Desai S. & Misra J.B. (2003) Genotypic differences and water-deficit induced enhancement in epicuticular wax load in peanut. *Crop Science* **43,** 1294–1299.

Seki M., Narusaka M., Abe H., Kasuga M., Yamaguchi-Shinozaki K., Carninci P., Hayashizaki Y. & Shinozaki K. (2001) Monitoring the expression pattern of 1300 *Arabidopsis* genes under drought and cold stresses by using a full-length cDNA microarray. *Plant Cell* **13,** 61–72.

Shepherd T. & Wynne Griffiths D. (2006) The effects of stress on plant cuticular waxes. *New Phytologists* **171,** 469–499.

Simpson C.E., Baring M.R., Schubert A.M., Black M.C., Melouk H.A. & Lopez Y. (2006) Registration of 'Tamrun OL 02' peanut. *Crop Science* **46,** 1813–1814.

Sun Z.W. & Allis C.D. (2002) Ubiquitination of histone H2B regulates H3 methylation and gene silencing in yeast. *Nature* **418,** 104–108.

Taylor N.L., Day D.A. & Millar A.H. (2002) Environmental stress causes oxidative damage to plant mitochondria leading to inhibition of glycine decarboxylase. *Journal of Boiological Chemistry* **277,** 42663–42668.

Taylor N.L., Heazlewood J.L., Day D.A. & Millar A.H. (2005) Differential impact of environmental stresses on the pea mitochondrial proteome. *Molecular & Cellular Proteomics* **4,** 1122–1133.

Tellmann G. & Geulen O. (2006) LightCycler® 480 Real-Time PCR system: innovative solutions for relative quantification. *Biochemica* **4,** 16–17.

Tezara W., Mitchell V.J., Driscoll S.D. & Lawlor D.W. (1999) Water stress inhibits plant photosynthesis by decreasing coupling factor and ATP. *Nature* **401,** 914–917.

Thornalley P. (1993) The glyoxalase system in health and disease. *Molecular Aspects of Medicine* **14,** 287–371.

Torres J.H., Chatellard P. & Stutz E. (1995) Isolation and characterization of *gmsti*, a stress-inducible gene from soybean (*Glycine max*) coding for a protein belonging to the TPR (tetratricopeptide repeats) family. *Plant Molecular Biology* **27,** 1221–1226.

United States Department of Agriculture Data and Statistics. (2006) [WWW document]. URL http://www.usda.gov/wps/portal/!ut/p/_s.7_0_A/7_0_1OB?navid=DATA_STATISTICS (accessed on 10 May 2007).

Upadhyaya H.D. (2005) Variability for drought related traits in the mini core collection of peanut. *Crop Science* **45,** 1432–1440.

Van Damme E.J.M., Barre A., Rougé P. & Peumans W.J. (2004) Cytoplasmic/nuclear plant lectins: a new story. *Trends in Plant Science* **9,** 484–489.

Watanabe T., Takeda A., Tsukiyama T., Mise K., Okuno T., Sasaki H., Minami N. & Imai H. (2006) Identification and characterization of two novel classes of small RNAs in the mouse germline: retrotransposon-derived siRNAs in oocytes and germline small RNAs in testes. *Genes & Development* **20,** 1732–1743.

Yoshida K.T., Wada T., Koyama H., Mizobuchi-Fukuoka R. & Naito S. (1999) Temporal and spatial patterns of accumulation of the transcript of myo-inositol-1-phosphate synthase and phytin-containing particles during seed development in rice. *Plant Physiology* **119,** 65–72.

Zhang J.Y., Broeckling C.D., Blancaflor E.B., Sledge M.K., Sumner L.W. & Wang Z.Y. (2005) Overexpression of WXP1, a putative *Medicago truncatula* AP2 domain-containing transcription factor gene, increases cuticular wax accumulation and enhances drought tolerance in transgenic alfalfa (*Medicago sativa*). *The Plant Journal* **42,** 689–707.

Zhang X., Liu S. & Takano T. (2008) Overexpression of a mitochondrialATP synthase small subunit gene (AtMtATP6) confers tolerance to several abiotic stresses in *Saccharomyces cerevisiae* and *Arabidopsis thaliana*. *Biotechnology Letters* **30,** 1289–1294.

Zörb C., Schmitt S., Neeb A., Karl S., Linder M. & Schubert S. (2004) The biochemical reaction of maize (*Zea mays* L.) to salt stress is characterized by a mitigation of symptoms and not by a specific adaptation. *Plant Science* **167,** 91–100.

Zuther E., Huang S., Jelenska J., *et al.* (2004) Complex nested promoters control tissue-specific expression of acetyl-CoA carboxylase genes in wheat. *Proceedings of the National Academy of Sciences of the United States of America* **101,** 1403–1408.

Received 18 November 2008; accepted for publication 5 December 2008

SUPPORTING INFORMATION

Additional Supporting Information may be found in the online version of this article:

Figure S1. Standardized protein extraction protocol from peanut leaf using phenol buffer.

Table S1. Primer list for qRT-PCR analysis of peanut genes.

Table S2. Peptide sequences of all hits for the proteins identified by 1-D shotgun of the excised bands 2A, 2B and 2C.

Please note: Wiley-Blackwell are not responsible for the content or functionality of any supporting materials supplied by the authors. Any queries (other than missing material) should be directed to the corresponding author for the article.